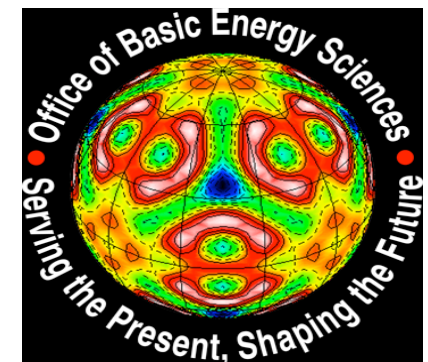


# Theory of Extremely Correlated Fermions (III-IV)

Collège de France  
April 9 2014

Sriram Shastry  
University of California  
Santa Cruz, CA



Work supported by  
DOE, BES DE-FG02-06ER46319

# Lightening Summary of last lecture

Usual Dyson type theory

$$\mathcal{G}(k, i\omega) \rightarrow \underbrace{\frac{1 - \frac{n}{2}}{i\omega + \mu - c \varepsilon_k - \Sigma(k, i\omega)}}_{\text{Dyson form}}$$

ECFL form gives instead:

$$\mathcal{G}(k, i\omega) = \underbrace{\frac{1}{i\omega + \mu - c\varepsilon_k - \Phi(k, i\omega)}}_{g(k, i\omega)} \times \underbrace{\left[1 - \frac{n}{2} + \Psi(k, i\omega)\right]}_{\mu(k, i\omega)}$$

auxiliary Greens function

caparison function

🕒 Calculation of the two self energies proceeds by one of three methods.

🕒 Expansion in parameter  $\lambda$  analogous to  $1/(2S)$  in spin wave theory, by a self consistent skeleton graph expansion (numerically implemented).

Formulas for self energies look like bubble graphs in Fermi liquid theory- self consistently lead to FL type behaviour

🕒 Phenomenological models for  $\Psi$  and  $\Phi$  based on Fermi liquid type hypothesis from the  $\lambda$  expansion

🕒 Low  $k, \omega$  expansion of the self energies  $\Psi$  and  $\Phi$ , inspired by the comparison with DMFT-

$$\Psi(k) = -2\lambda \sum_{p,q} E(k, p) \mathbf{g}(p) \mathbf{g}(q) \mathbf{g}(q + p - k),$$

$\Phi =$  [diagram 1] + [diagram 2] + [diagram 3] + ...  
 $\Psi =$  [diagram 4] + [diagram 5] + ...  
 $\rightarrow \equiv g$      $\sim = (t+J)$   
 $\dots = 1$

$$\bar{\Phi}(k) = -2\lambda \sum_{p,q} E(k, p) [E(p, k) + E(q + p - k, p)] \times \mathbf{g}(p) \mathbf{g}(q) \mathbf{g}(q + p - k).$$

Phenomenological spectral function s-ECFL  
(Shastry PRL 2011, Gweon et al PRL 2011)

$$\Psi(\omega) \sim -\frac{1}{\Delta} \Phi(\omega)$$

Dimensional/engineering approximation  
of  $O(\lambda^2)$  equations.

$$\Phi(\omega) = \int dx \frac{\Gamma(x)}{i\omega - x}$$

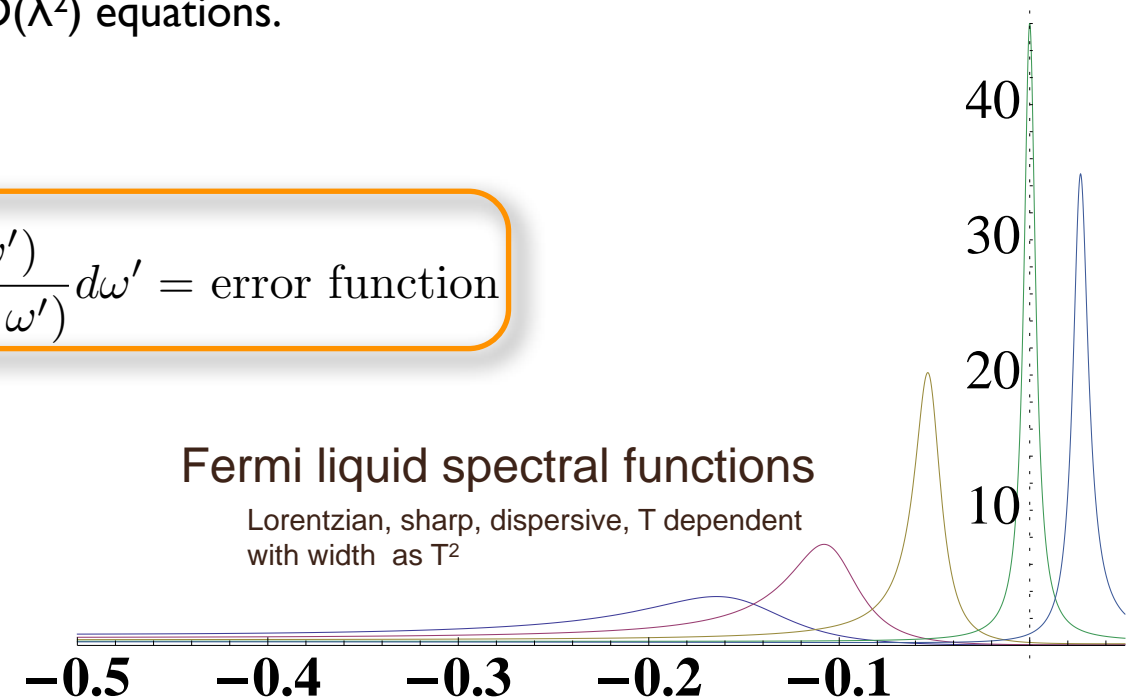
$$\Gamma(\omega) = \frac{\omega^2 + \pi^2 T^2}{\omega_0} e^{-(\pi^2 T^2 + \omega^2)/\Omega_0^2}$$

$$h(\omega) = \mathcal{P} \int \frac{\Gamma(\omega')}{(\omega - \omega')} d\omega' = \text{error function}$$

$$A_{FL}(\omega) = \frac{\Gamma(\omega)}{\Gamma^2(\omega) + (\omega - \hat{k}v_F - h(\omega))^2}$$

$$A_{sECFL}(\omega) = \frac{1}{\pi} \frac{\Gamma(\omega)}{\Gamma^2(\omega) + (\omega - \hat{k}v_F - h(\omega))^2} \times \left(1 - \frac{\omega}{\Delta} + c\hat{k}v_F\right)$$

Remarkably light description  
with only three parameters: (c is fixed,  $\Delta$  computed).  
1)  $\eta$  (Impurity scattering- extrinsic) so that  $\Gamma \rightarrow \Gamma + \eta$ .  
(needed for Laser vs synchrotron ARPES)  
2)  $\Omega_0$  (strength of FL)  
3)  $\omega_0$  (High frequency cut off of FL)



$$\Delta = \int d\omega f(\omega) \langle A_{FL}(k, \omega) (\epsilon - \mu - \omega) \rangle_k$$

Expand both the self energies at small  $(k, \omega)$  assuming a Fermi liquid structure.

Long wavelength expansion

$$1 - \frac{n}{2} + \Psi(\vec{k}, \omega) = \alpha_0 + c_\psi (\omega + v_\psi \hat{k} v_f) + i\mathcal{R}/\gamma_\psi + O(\omega^3)$$

$$\omega + \mu - \left(1 - \frac{n}{2}\right) \varepsilon_k - \Phi(k, \omega) = (1 + c_\phi) \left(\omega - v_\phi \hat{k} v_f + i\mathcal{R}/\Omega_\phi + O(\omega^3)\right)$$

$$\alpha_0 = 1 - \frac{n}{2} + \Psi_0 \rightarrow (1 - n)$$

$$\mathcal{R} = \pi \{\omega^2 + (\pi k_B T)^2\}$$

$$\hat{k} = (\vec{k} - \vec{k}_F) \cdot \vec{k}_F / |\vec{k}_F|$$

$$v_f = (\partial_k \varepsilon_k)_{k_F} \text{ is the bare Fermi velocity}$$

Non Lorentzian Spectral function with **5** parameters

$$A(\vec{k}, \omega) = \frac{z_0}{\pi} \frac{\Gamma_0}{(\omega - v_\phi \hat{k} v_f)^2 + \Gamma_0^2} \times \mu(k, \omega)$$

$$\Gamma_0(\hat{k}, \omega) = \eta + \frac{\pi(\omega^2 + (\pi k_B T)^2)}{\Omega_\phi}$$

$$\mu(\hat{k}, \omega) = 1 - \frac{\omega}{\Delta_0} + \frac{v_0 \hat{k} v_f}{\Delta_0}$$

$$\{\Delta_0, z_0, \Omega_\phi, \nu_0, \nu_\phi\} \quad v_F \rightarrow \text{bare Fermi velocity}$$

Comments:

● Notable feature of all the ECFL spectral functions is the non Lorentzian nature- due to the multiplying factor (caparison factor) that depends on  $k$  and  $\omega$ .

● As a result different “spectra”- locating the maxima of  $A(k,\omega)$ -are definable:

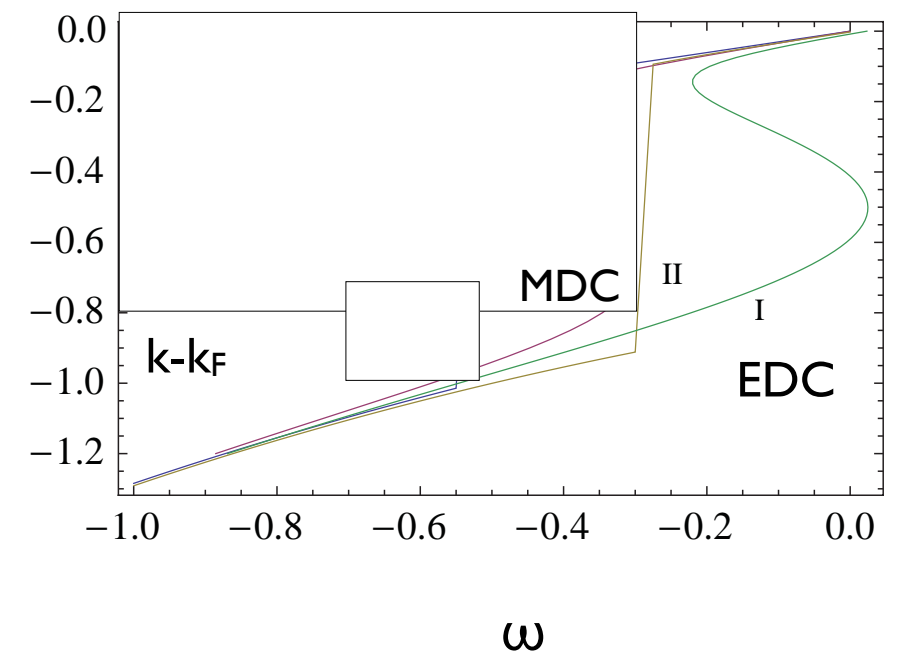
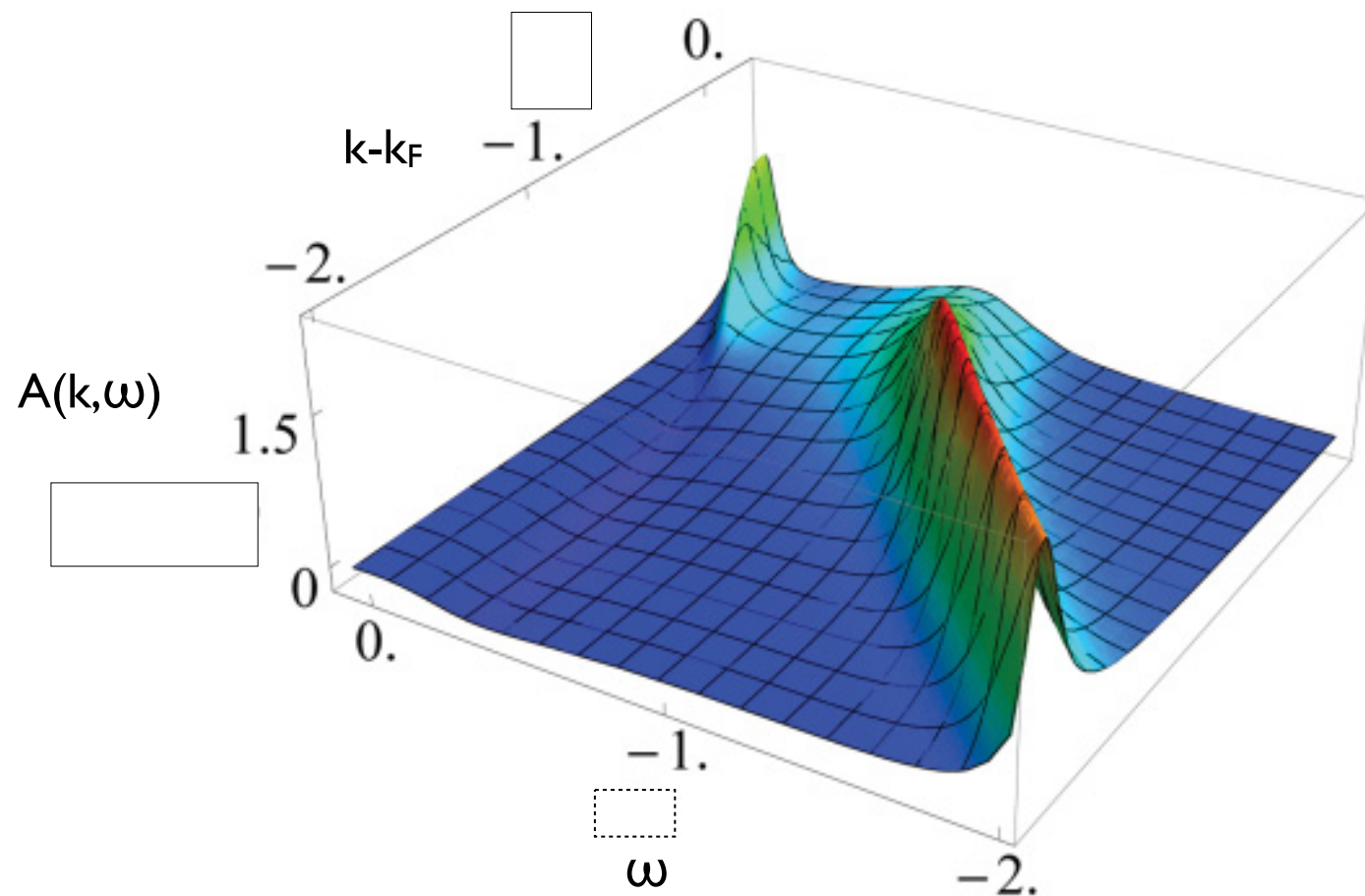
● at fixed  $k$  scan various  $\omega$  (EDC's)

● at fixed  $\omega$  scan versus  $k$  (MDC's)

● The MDC spectrum and EDC spectrum differ at very low energies in the spectral function  $A_{ECFL}(k,\omega)$ - the caparison factor makes the difference.

● The story has a parallel in neutron scattering, See- *the notorious case of spin waves in Iron above  $T_c$ , (1978-81)*.

● Here locating *spin waves* from constant  $k$  scans is right, often constant  $\omega$  scans were used to make dramatic, but ultimately incorrect claims.



## Theoretical Results and Benchmarking

- Short summary of second order results in 2-dimensions
- Comparison with High T expansion results
- Comparison with DMFT
- Comparison with Anderson Impurity Model

## Experimental Benchmarking and predictions

- ARPES Line shapes: ECFL
  - ARPES Line shapes+ Casey Anderson theory
  - ARPES High energy kinks- ( $t-t'-J$  model electron doped versus hole doping)
  - ARPES Low energy kinks from ECFL
- ASYMMETRY- emergent energy scale- its identification and isolation as an urgent task

## Open questions

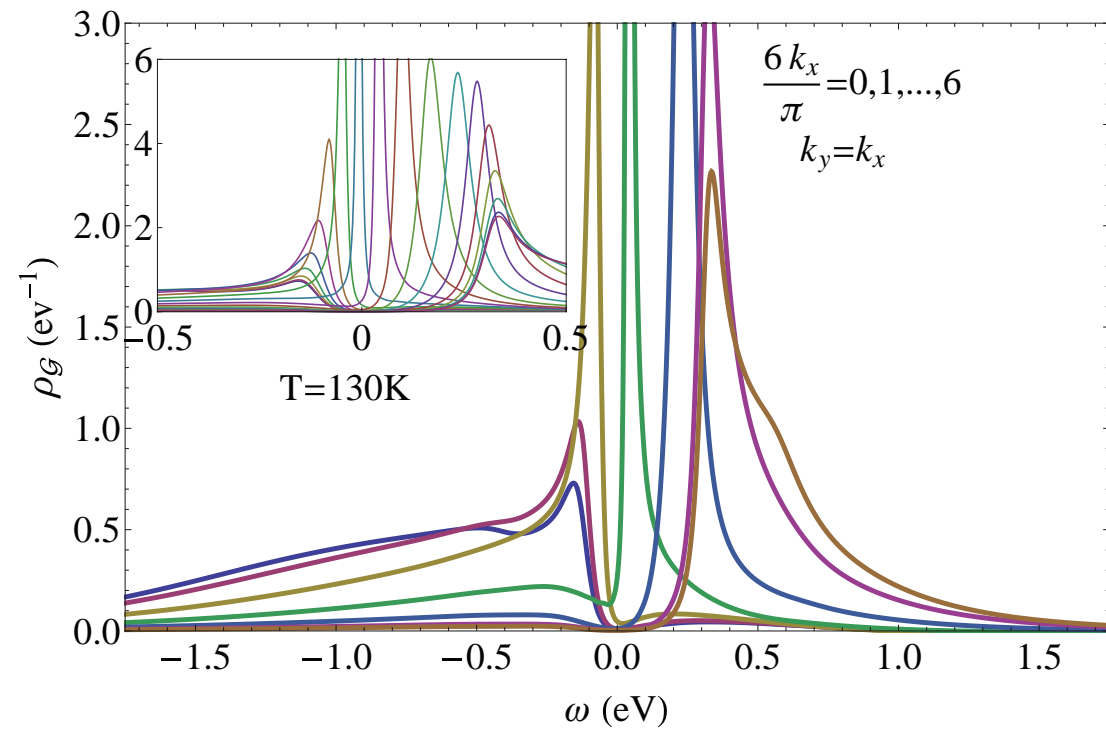
# Short summary of second order results in 2-dimensions

PHYSICAL REVIEW B **87**, 245101 (2013)

## Extremely correlated Fermi liquids: Self-consistent solution of the second-order theory

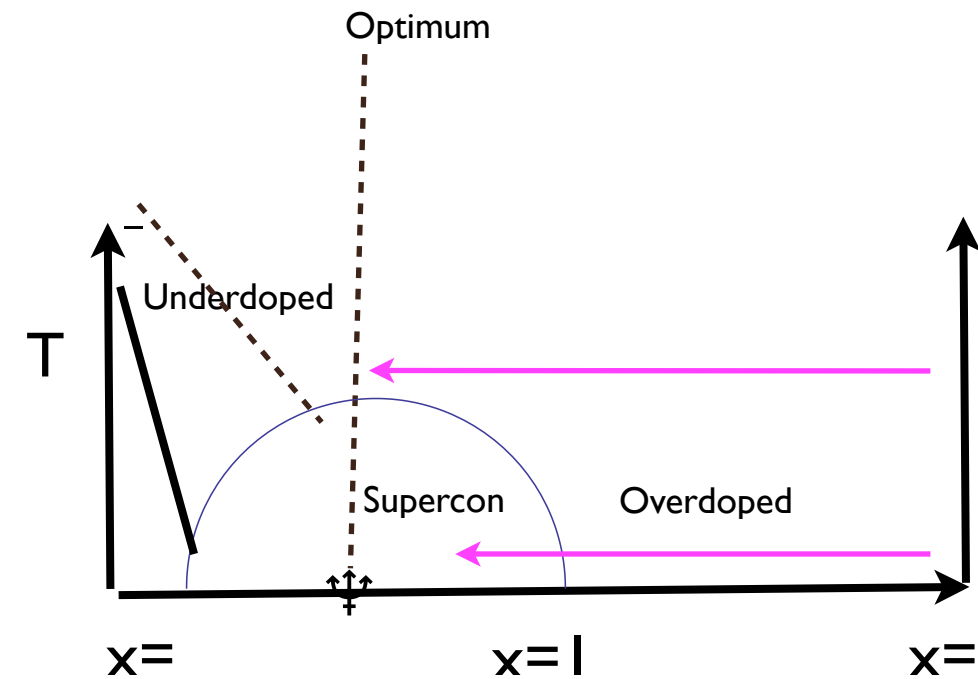
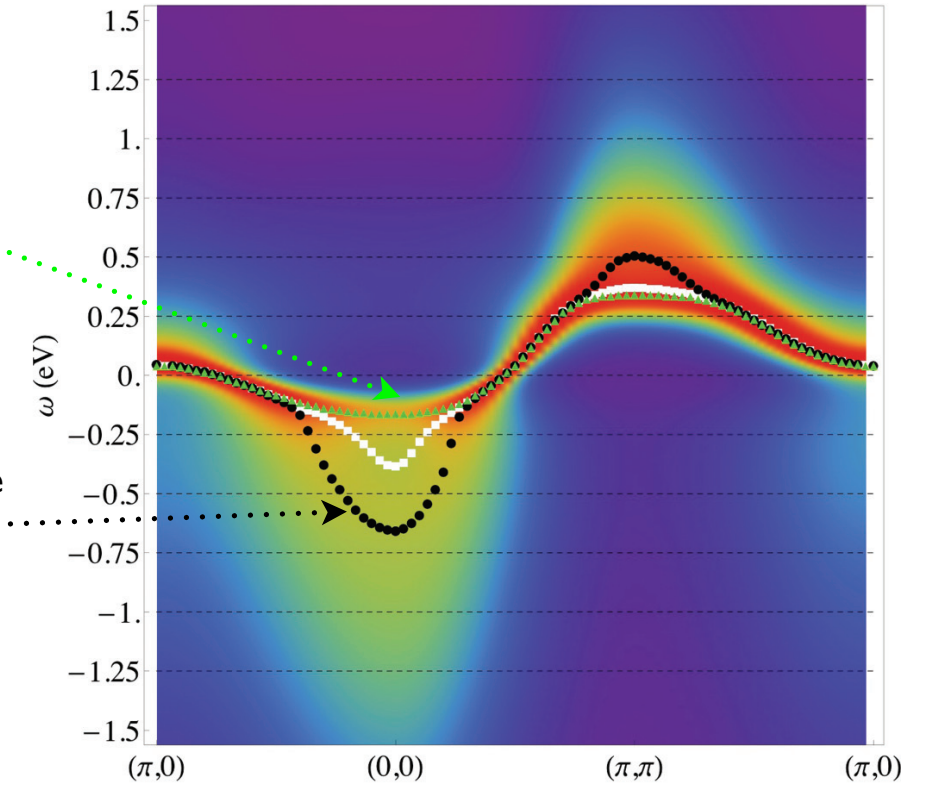
Daniel Hansen and B. Sriram Shastry

$$\rho_G(k, \omega) \equiv A(k, \omega)$$



EDC spectra everywhere  
in Green dots

MDC spectra everywhere  
in Black dots



→  
Here the electron doped case,  
modeled by  $t'/t = -.4$  has a larger  
feature, as in experiments!

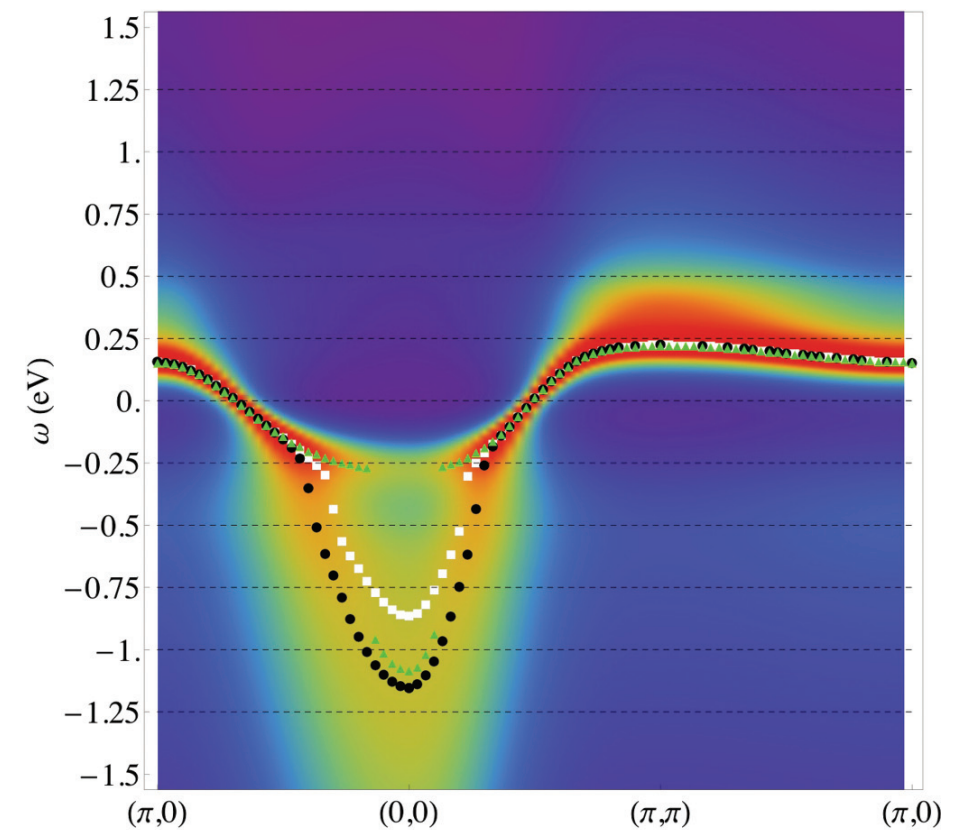


FIG. 3. (Color online)  $L = 60$  ( $n = T = 0.75 - 300$ ) K. Density

# Comparison with High T expansion results

PHYSICAL REVIEW B **87**, 161120(R) (2013)

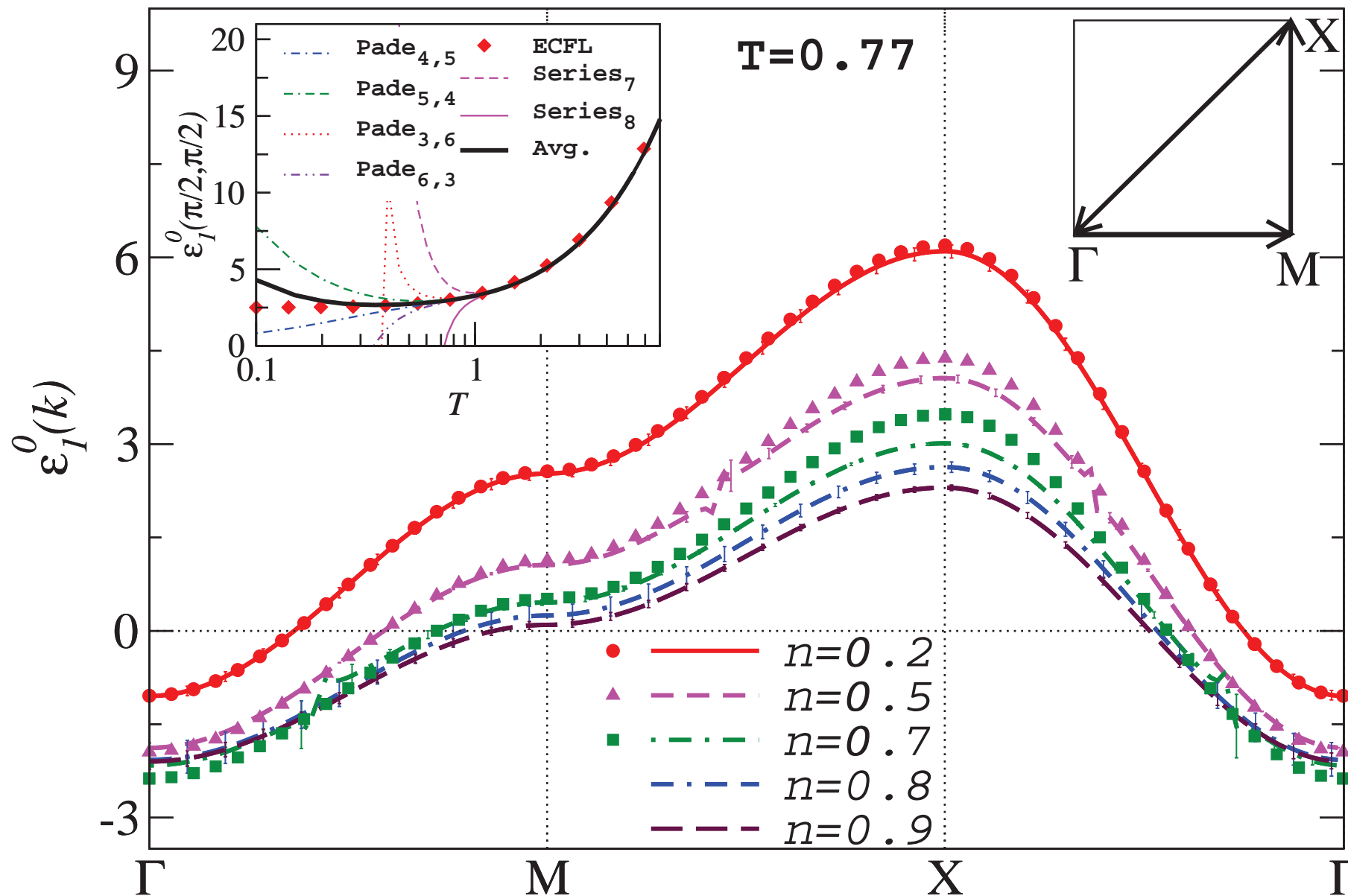
## Electronic spectral properties of the two-dimensional infinite- $U$ Hubbard model

Ehsan Khatami,<sup>1,2</sup> Daniel Hansen,<sup>1</sup> Edward Perepelitsky,<sup>1</sup> Marcos Rigol,<sup>3</sup> and B. Sriram Shastry<sup>1</sup>

Dynamics out to quite high (8<sup>th</sup>) order in hopping computed, using Metzner's series for  $G$ .

$$\varepsilon_1^0(k) = \frac{\langle \{ [\hat{C}(k), H], \hat{C}^\dagger(k) \} \rangle}{\langle \{ \hat{C}(k), \hat{C}^\dagger(k) \} \rangle}$$

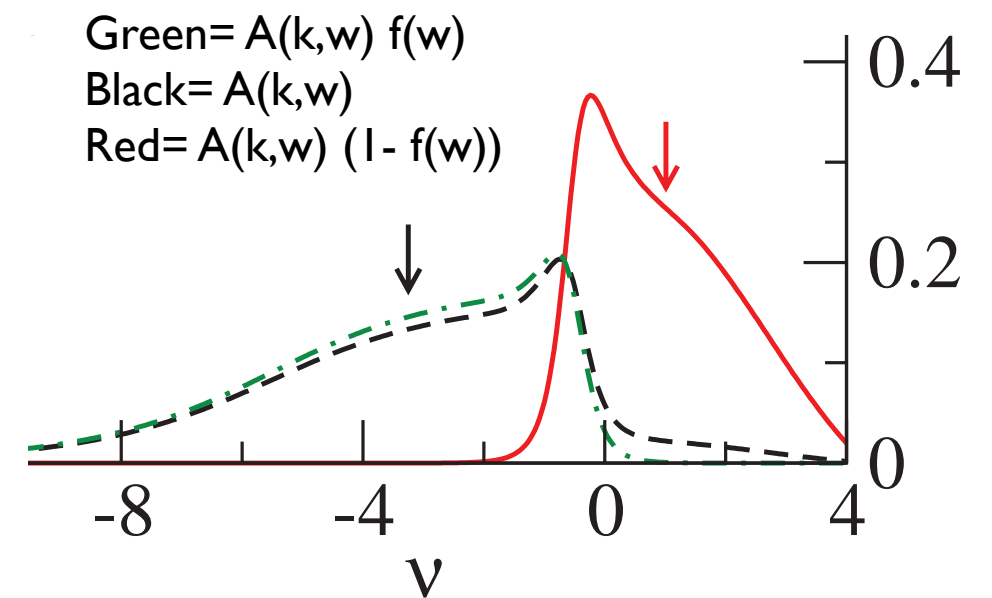
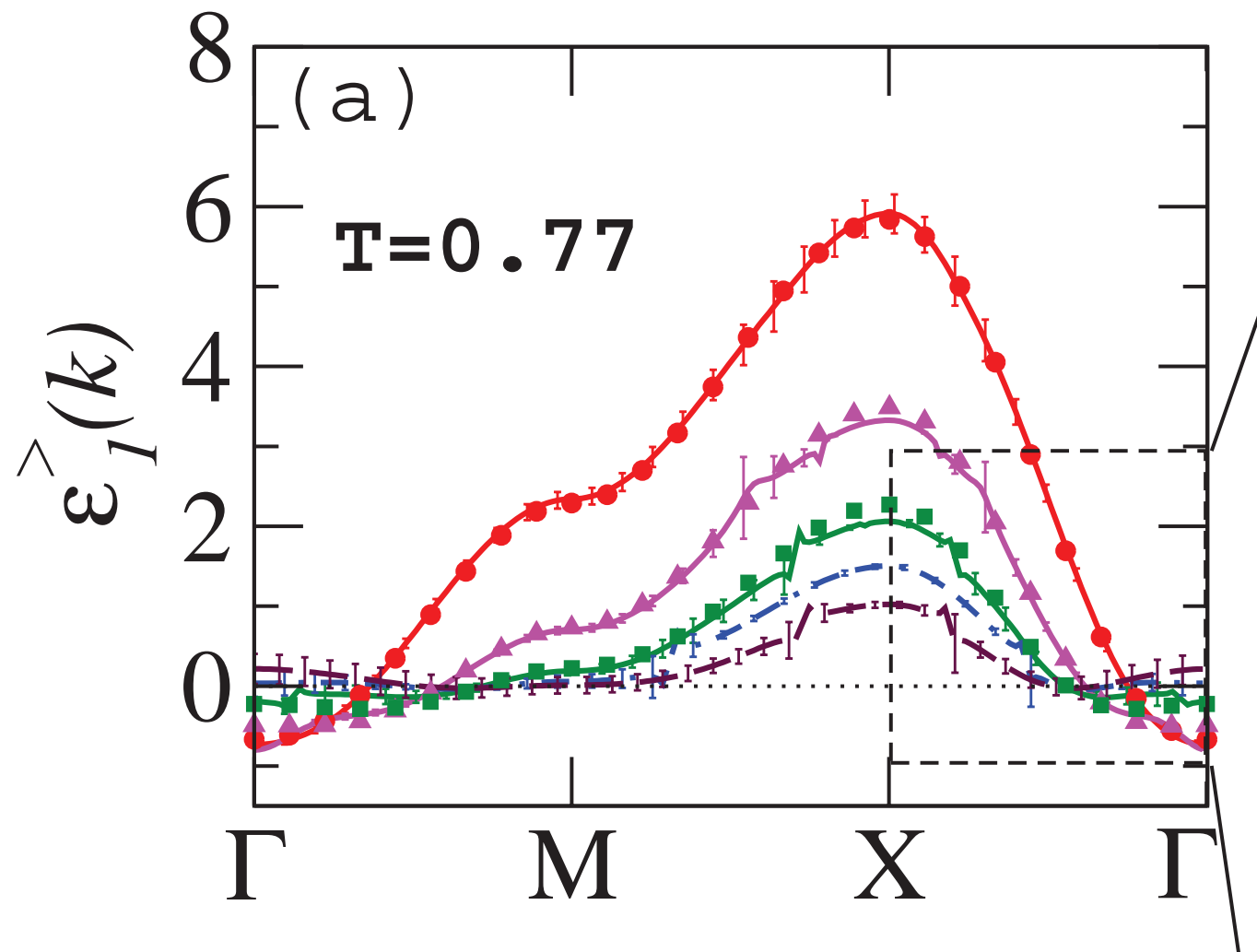
Symmetric moment (EDC) can be compared with ECFL spectrum to  $O(\lambda^2)$ , and does quite well except at high energy (unoccupied) states near X point



← Here ECFL is the symbols and Pade results as solid/dashed lines- up to  $n \sim 0.7$ . Beyond  $n \sim 0.7$  ECFL is not available and only series results are shown.

$$\varepsilon_1^>(k) = \frac{\langle [\hat{C}(k), H] \hat{C}^\dagger(k) \rangle}{\langle \hat{C}(k) \hat{C}^\dagger(k) \rangle}$$

Particle addition type moment does much better.  
Essentially exact agreement with the actual QP peaks.  
Reason is that unoccupied Fermi function invoked here kills the long tails in the occupied side (see ECFL curves), and thereby focuses on the QP's.



Compare with DMFT in infinite D  
Formal preliminaries

Extremely correlated Fermi liquids in the limit of infinite dimensions

Edward Perepelitsky\*, B. Sriram Shastry

Annals of Physics 338 (2013) 283–301

In high dimensions we can show that these are further related through

$$\Psi(k) = \Psi(i\omega_k),$$

$$\Phi(k) = \chi(i\omega_k) + \epsilon_k \Psi(i\omega_k).$$

$$\Sigma_{DM}(k) = \Sigma_{DM}(i\omega_k) = \frac{(i\omega_k + \mu)\Psi(i\omega_k) + \left(1 - \frac{n}{2}\right)\chi(i\omega_k)}{1 - \frac{n}{2} + \Psi(i\omega_k)},$$

$$\Psi(i\omega_k) = -\lambda u_0 I_{000}(i\omega_k) + 2\lambda I_{010}(i\omega_k),$$

$$\chi(i\omega_k) = -\frac{u_0}{2}\Psi(i\omega_k) - u_0 \lambda I_{001}(i\omega_k) + 2\lambda I_{011}(i\omega_k).$$

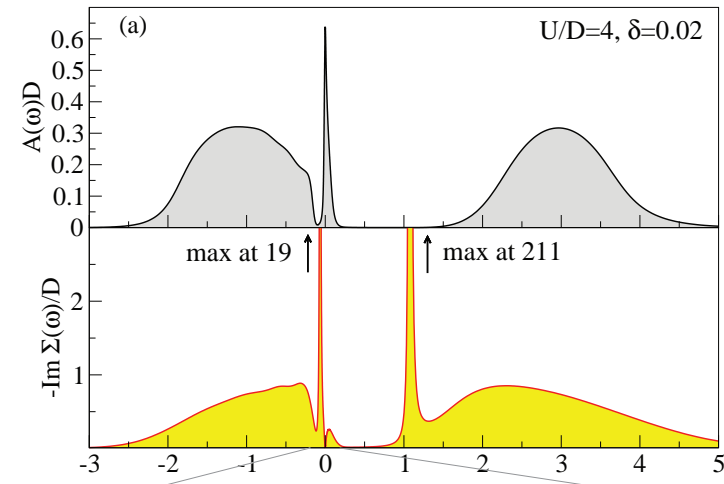
$$\mathbf{g}_{\text{loc},m}(i\omega_k) \equiv \sum_{\vec{k}} \mathbf{g}(k) \epsilon_{\vec{k}}^m,$$

$$I_{m_1 m_2 m_3}(i\omega_k) \equiv - \sum_{\omega_p, \omega_q} \mathbf{g}_{\text{loc},m_1}(i\omega_q) \mathbf{g}_{\text{loc},m_2}(i\omega_p) \mathbf{g}_{\text{loc},m_3}(i\omega_q + i\omega_p - i\omega_k),$$

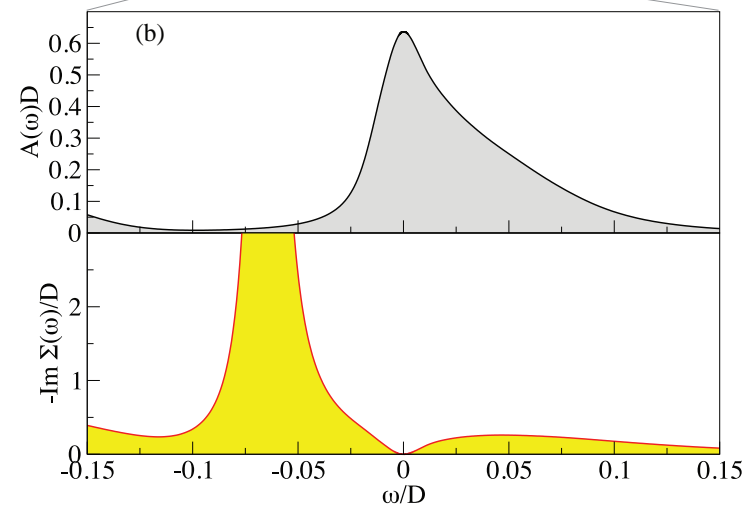
$$\sum_k \mathbf{g}(k) = \frac{n}{2}; \quad \sum_k \mathcal{G}(k) = \frac{n}{2}.$$

# Extremely correlated Fermi liquid theory meets dynamical mean-field theory: Analytical insights into the doping-driven Mott transition

R. Žitko,<sup>1,2</sup> D. Hansen,<sup>3</sup> E. Perepelitsky,<sup>3</sup> J. Mravlje,<sup>1</sup> A. Georges,<sup>4,5,6</sup> and B. S. Shastry<sup>3</sup>



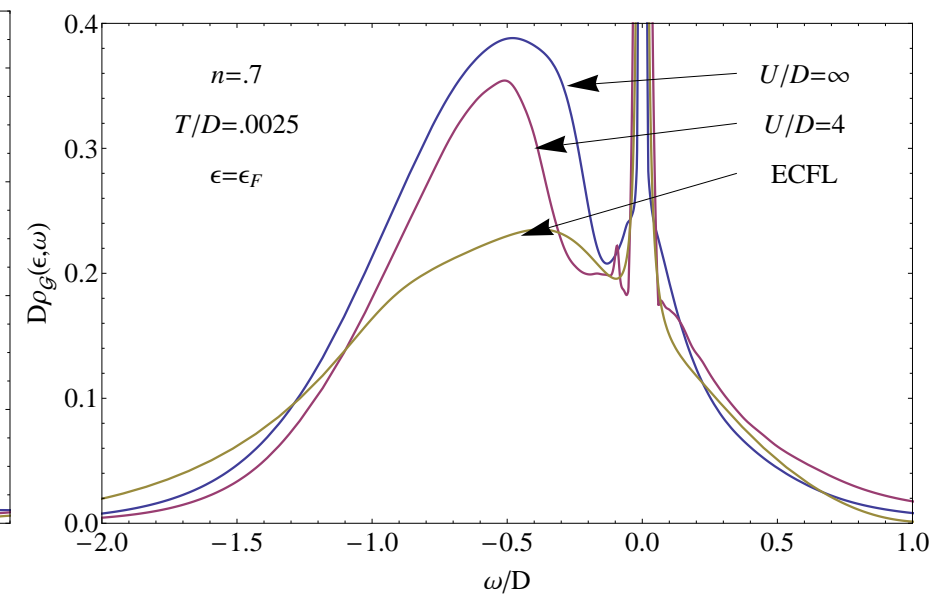
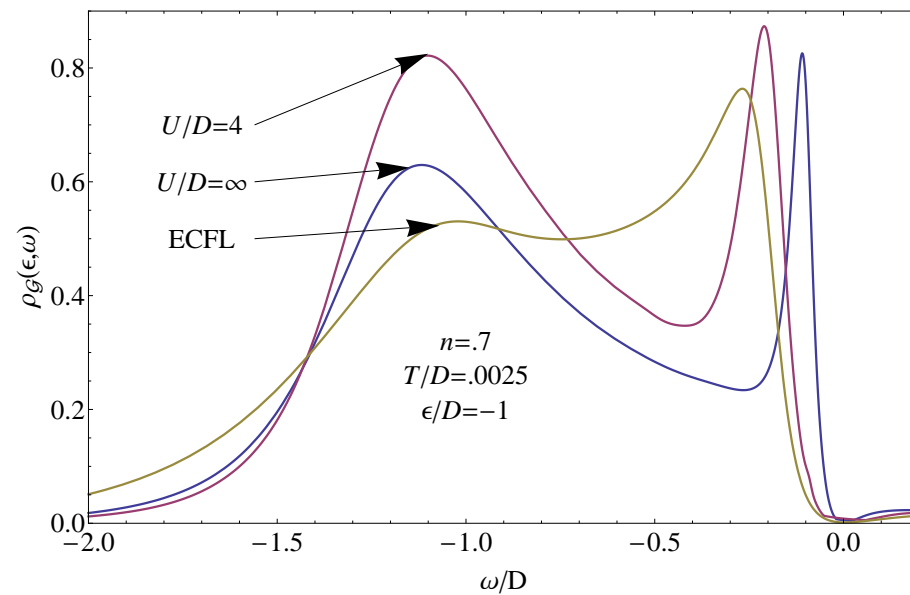
Very high precision low-T DMFT results for local spectral function (k-averaged) and Imaginary self energy



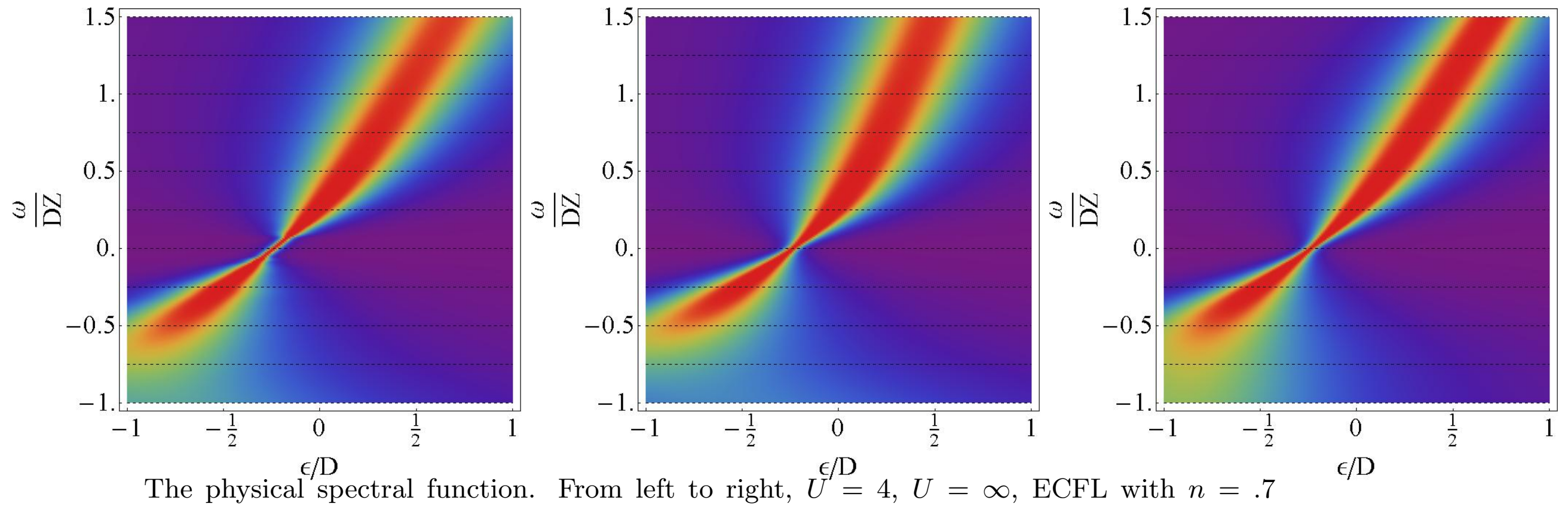
Same picture zooming into low  $\omega$ .

Absolute scale comparison of ECFL and DMFT at different energies.

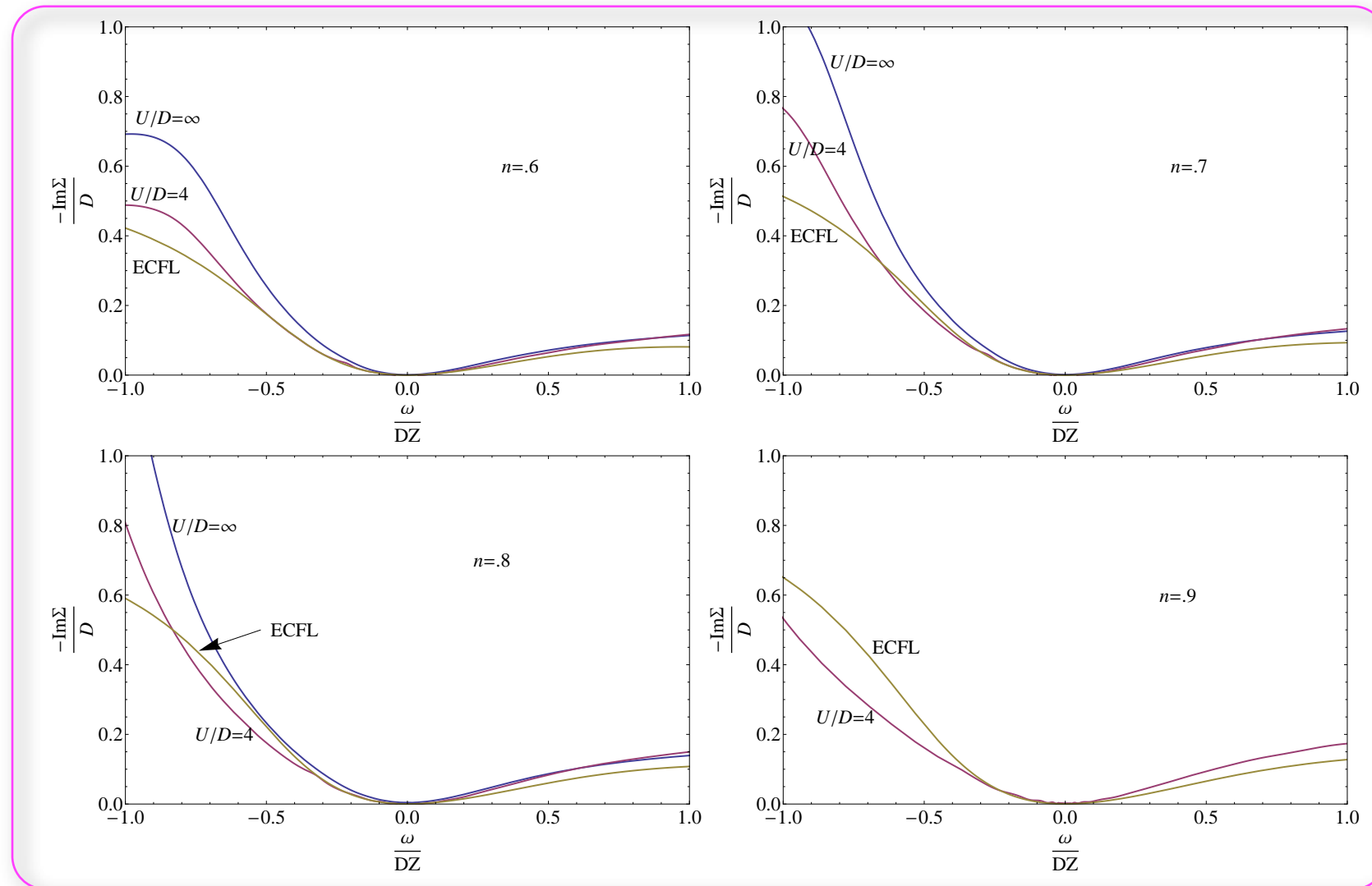
$\epsilon = -D$  (left) and  $\epsilon = 0$  (right).



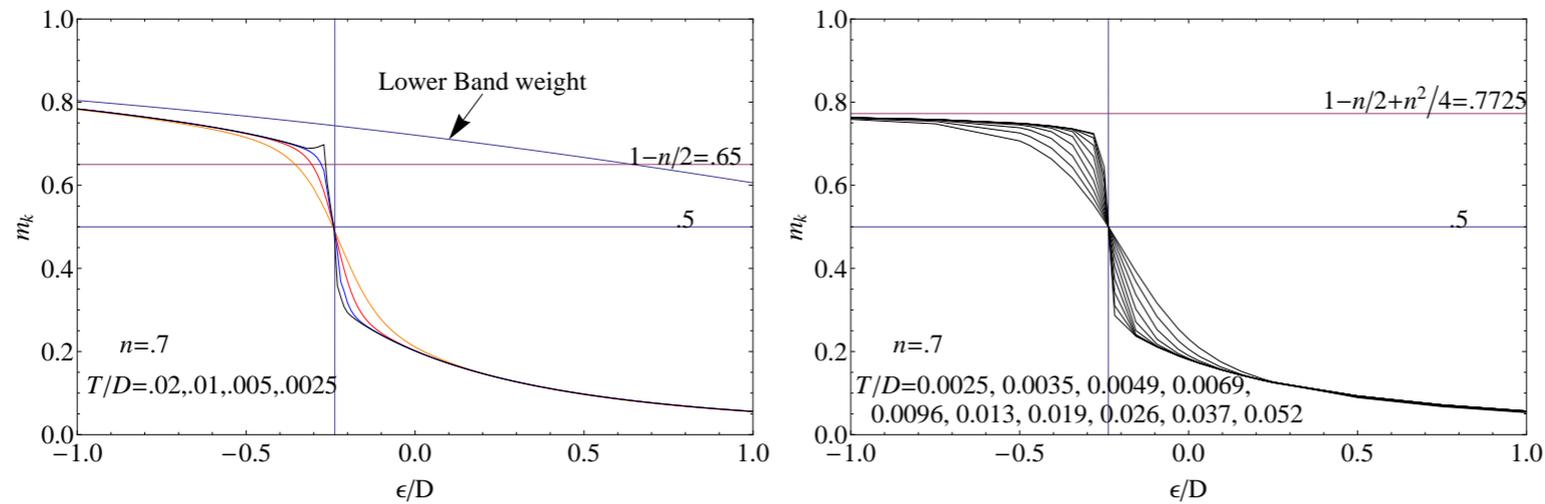
A comparison of ECFL and DMFT spectral function color plots after scaling the frequency by Z (the QP weight). In this rough representation, it is hard to tell the theories apart!



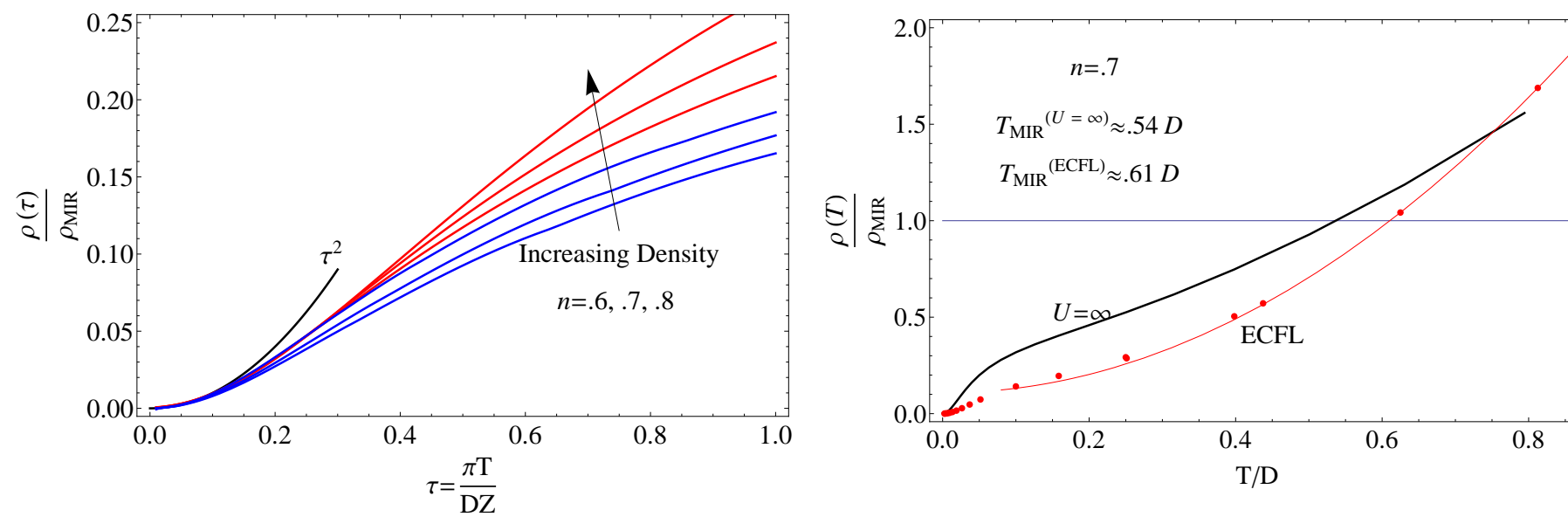
## A comparison of ECFL and DMFT after scaling the frequency by $Z$ (the QP weight).



- 🌟 The  $O(\lambda^2)$  version of ECFL used here seems closer to  $U=4D$ , consistent with the interpretation of  $\lambda$ .
- 🌟 The shapes of the functions are in excellent accord- out to unexpectedly high densities- (ECFL version arguably good for small densities, does impressively well at high densities.)
- 🌟 Note the strong particle hole asymmetry about  $\omega=0$ . A strong bias in both theories- discussed later.



Momentum Occupation vs  $\epsilon$  with DMFT and ECFL on left and right, respectively



Exciting because we obtain a promising synthesis between the analytical power of ECFL and the exact numerical power of DMFT. Much more to learn from this joint approach.....

Anderson Impurity Model  
 ECFL at  $O(\lambda^2)$  compared to Wilson's Numerical Renormalization Group  
 at infinite  $U$

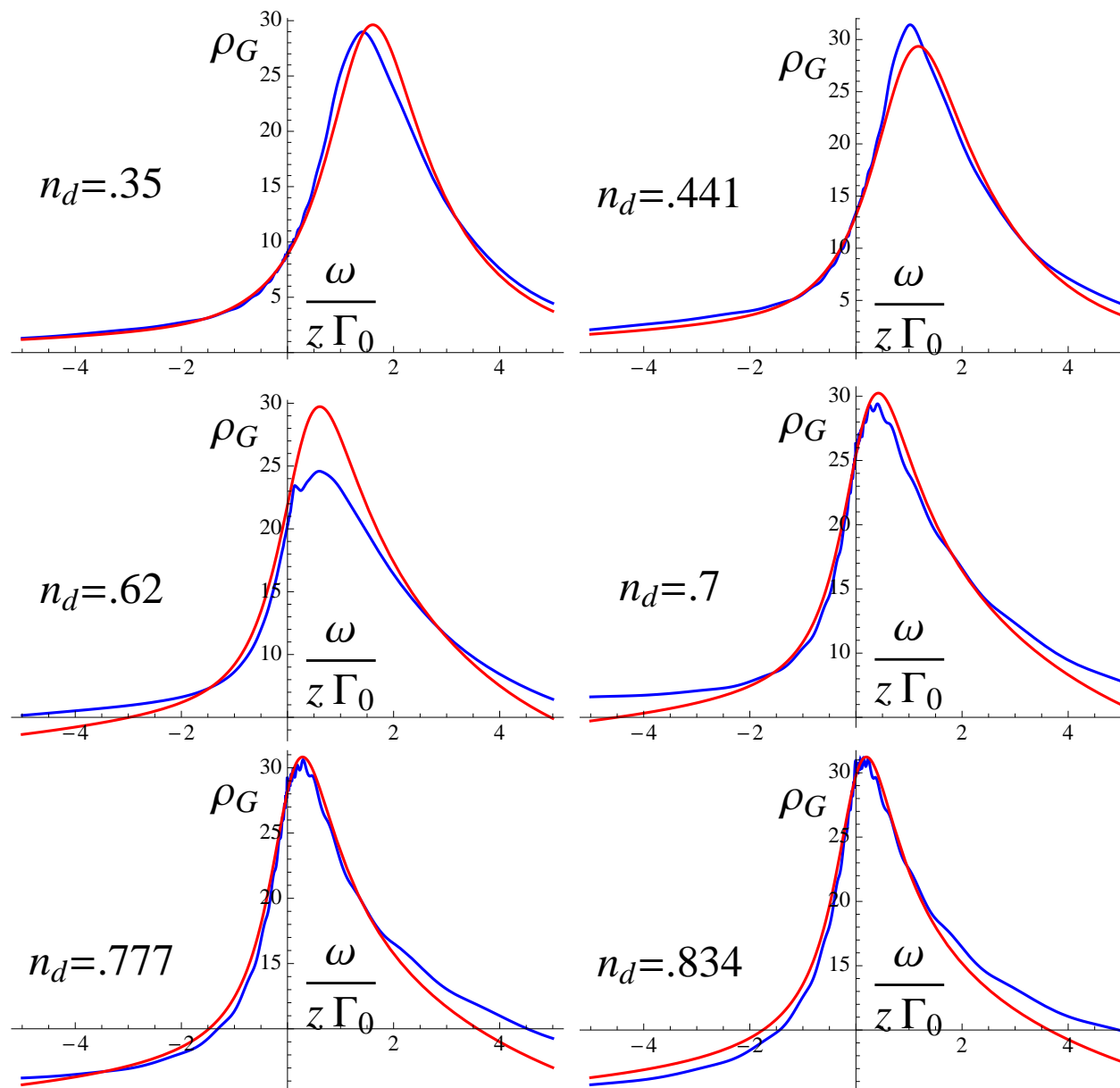
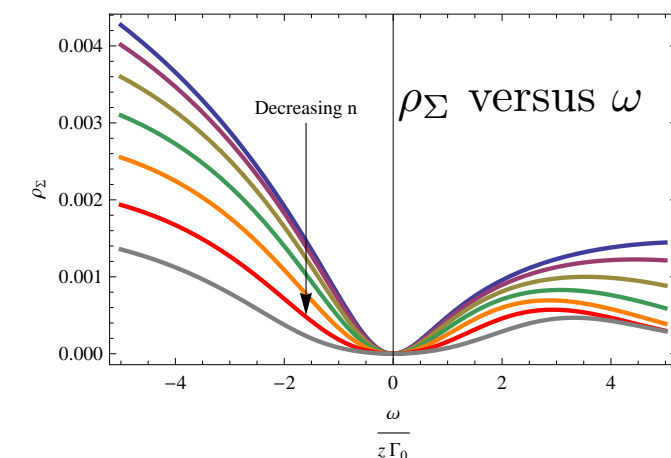
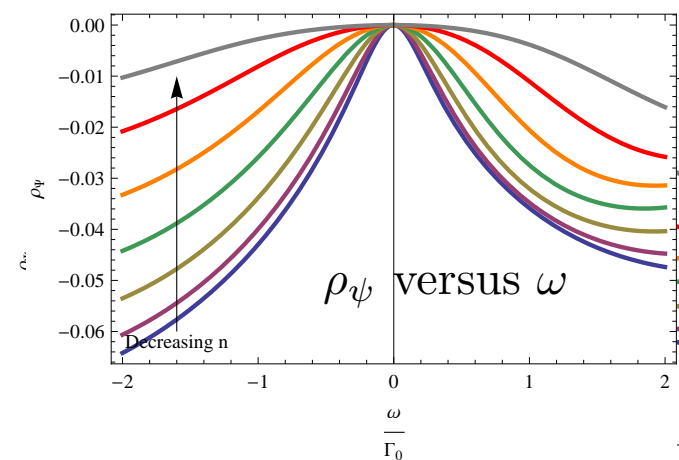
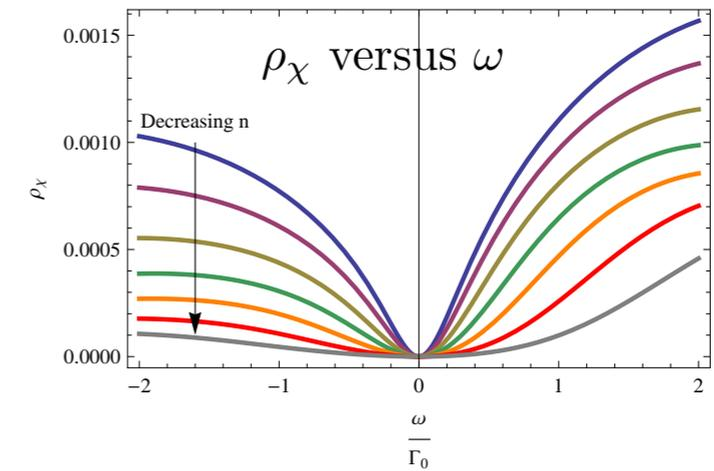
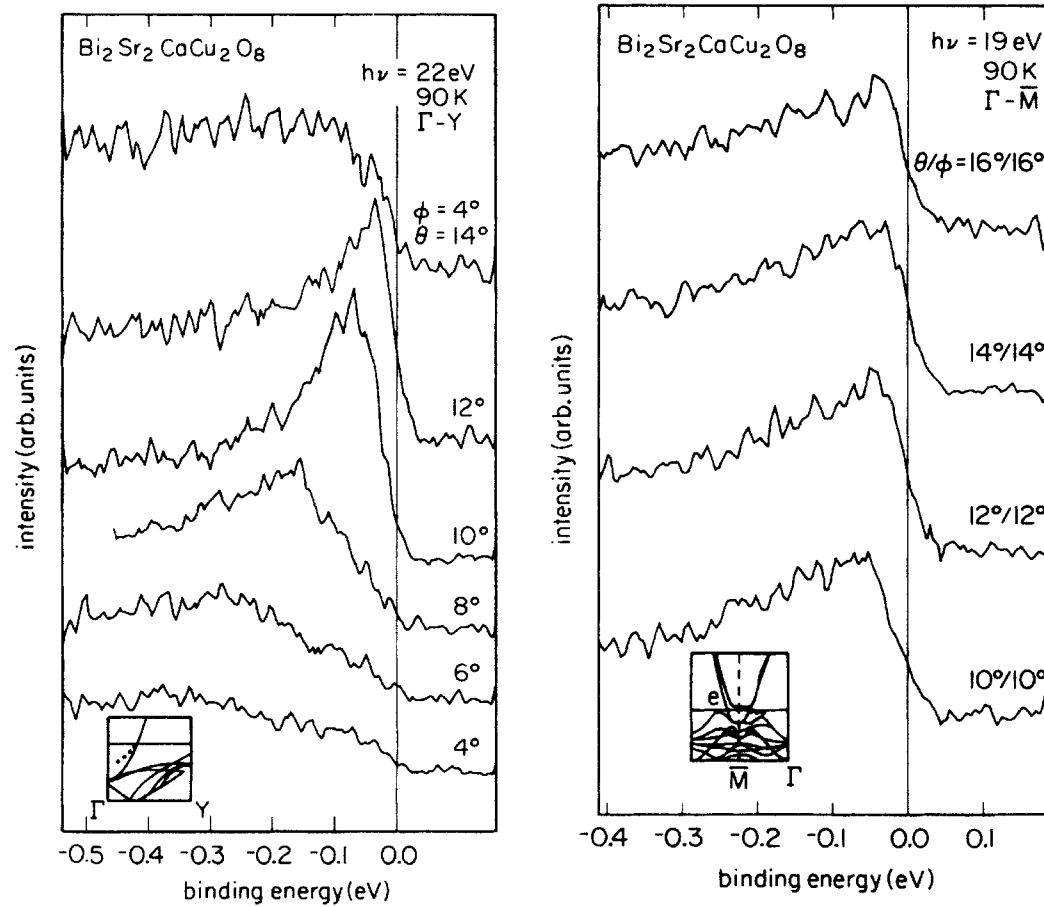


FIG. 1. The spectral density for the physical Green's function versus  $\frac{\omega}{\Gamma_0 z}$  for densities of  $n_d = .35, .441, .62, .7, .777, .834$ . The red curve is the ECFL calculation, while the blue curve is the NRG calculation.



# Angle resolved photo emission ARPES (1990) Surprising.



High-resolution angle-resolved photoemission study of the Fermi surface and the normal-state electronic structure of  $\text{Bi}_2\text{Sr}_2\text{CaCu}_2\text{O}_8$

C. G. Olson, R. Liu, and D. W. Lynch

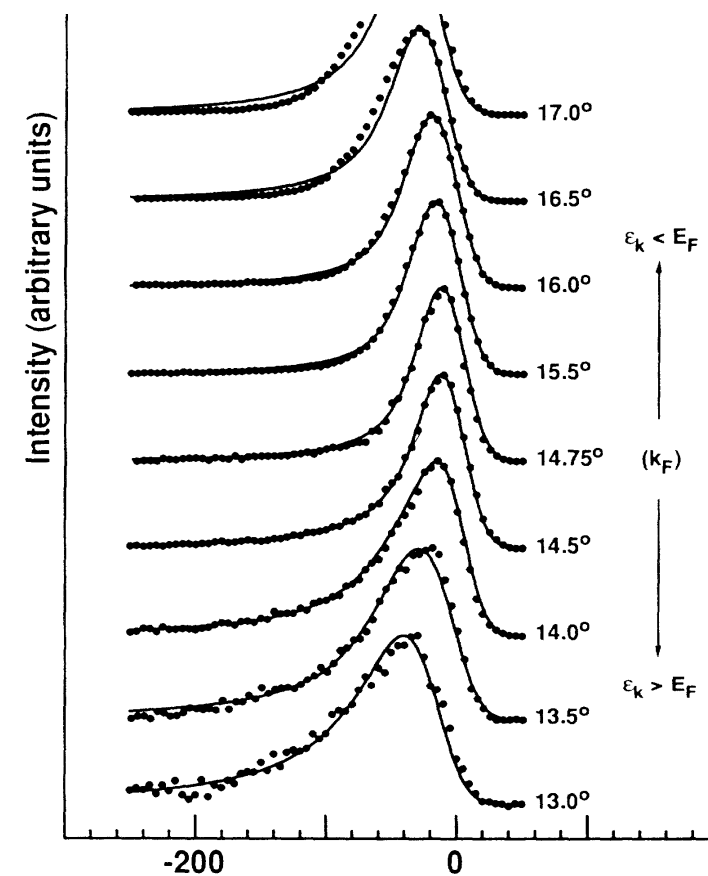
$$I_{ARPES} \sim |M|^2 \times A(k, \omega) \times f(\omega)$$

$$A(k, \omega) = \sum_{\alpha, \nu} e^{-\beta \varepsilon_\alpha} |\langle \nu | C(k) | \alpha \rangle|^2 \delta(\omega + \varepsilon_\nu - \varepsilon_\mu)$$

$$A_{FL}(k, \omega) \sim \frac{\Gamma/\pi}{\Gamma^2 + (\omega - E_k)^2}$$

$$\Gamma_{FL} \sim (\omega^2 + \pi^2 T^2)$$

$E_k$  = Quasi hole energy



Fermi-Liquid Line Shapes Measured by Angle-Resolved Photoemission Spectroscopy on 1-T-TiTe<sub>2</sub>

R. Claessen, R. O. Anderson, and J. W. Allen  
Randall Laboratory, University of Michigan, Ann Arbor, Michigan 48109-1120

C. G. Olson and C. Janowitz

Casey Anderson (2010)  
 Doniach Sunjic- Nozieres de Dominicis (1968)

LETTERS

P.W. Anderson and P Casey  
 Hidden Fermi Liquid:  
 Beautiful and compact idea based on X ray  
 edge singularity work.

Accurate theoretical fits to laser-excited  
 photoemission spectra in the normal phase  
 of high-temperature superconductors

PHILIP A. CASEY<sup>1</sup>, J. D. KORALEK<sup>2,3</sup>, N. C. PLUMB<sup>2</sup>, D. S. DESSAU<sup>2,3</sup> AND PHILIP W. ANDERSON<sup>1\*</sup>

$$G(k, \omega) = \int \int dx dt e^{i(kx - \omega t)} t^{-p} / (x - v_F t).$$

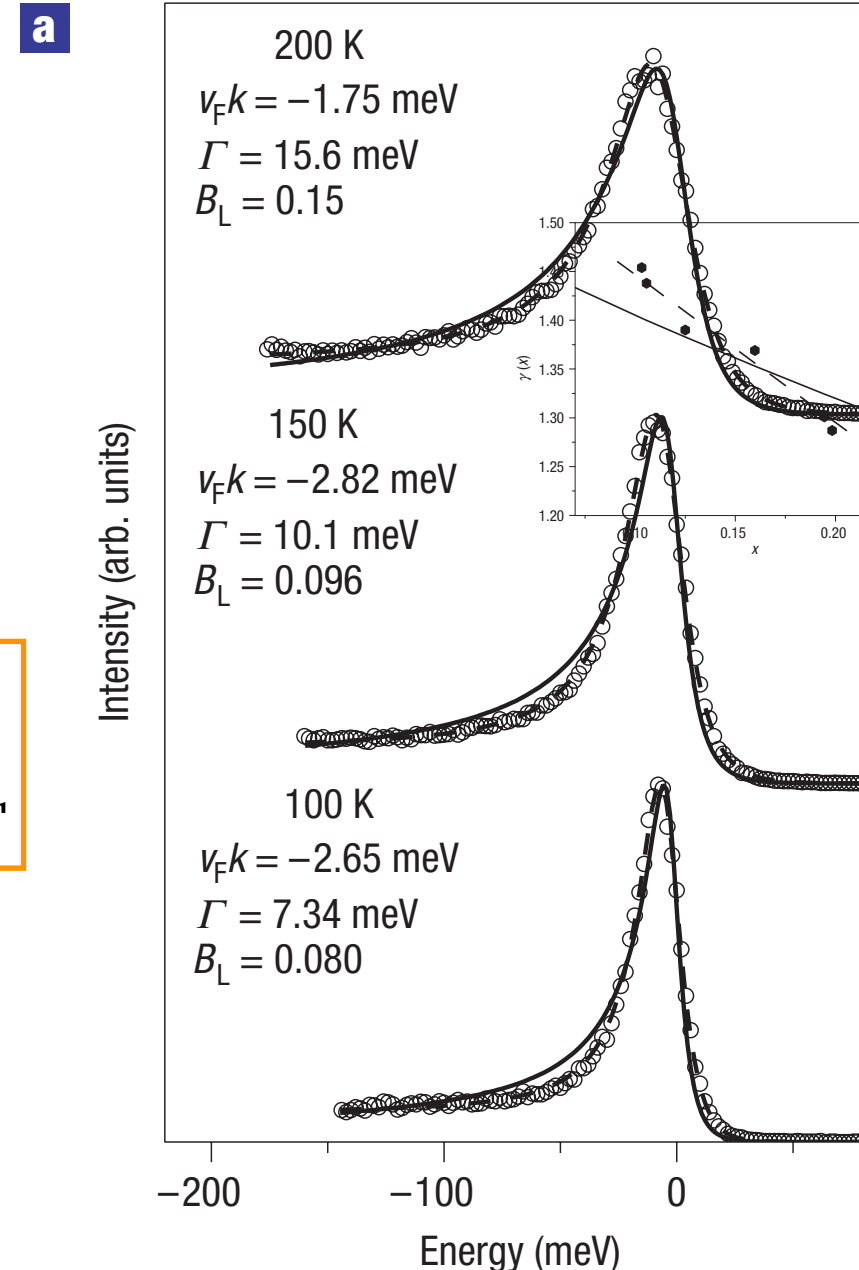
$$= \int dt t^{-p} e^{i(v_F k - \omega)t} \propto (v_F k - \omega)^{-1+p}.$$

$$p = \frac{1}{4} n^2$$

$$A(k, \omega) = f(\omega/T) \frac{\sin[(1-p)(\pi/2 - \tan^{-1}[(\omega - v_F k)/\Gamma])]}{[(\omega - v_F k)^2 + \Gamma^2]^{(1-p)/2}}.$$

$$\Gamma = aT$$

At T=0 is a Non Fermi Liquid at any  
 density n.  
 At finite T looks a lot like ECFL  
 because it has the right asymmetry  
 built into it



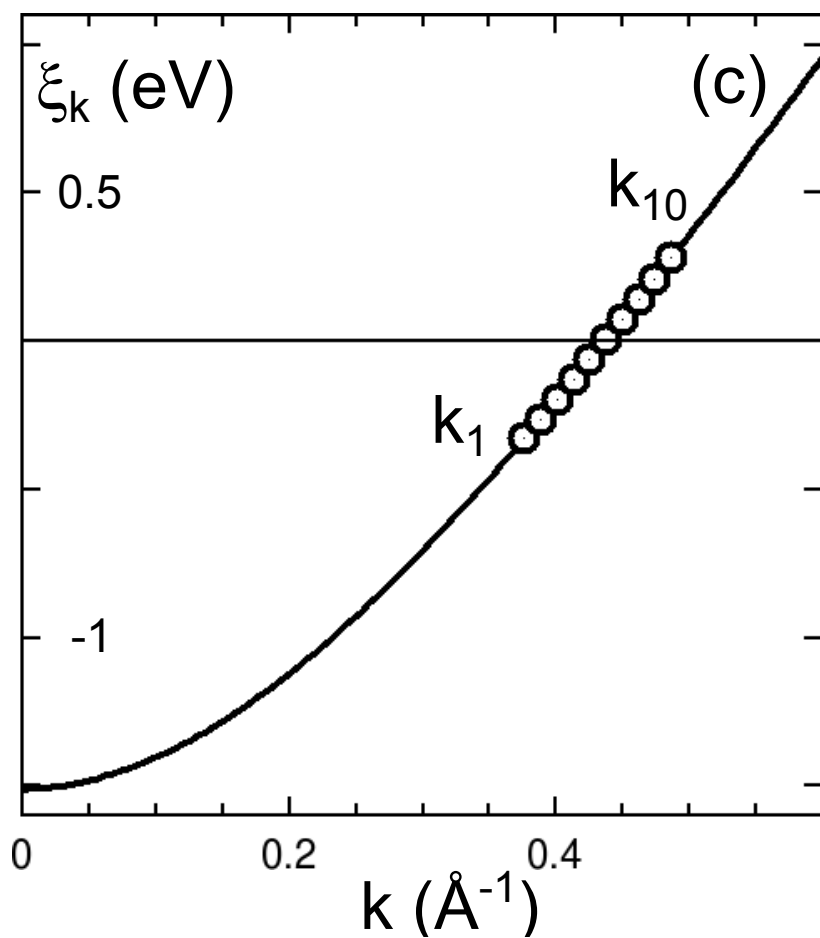
# Simplified ECFL 3 parameter fn vs data:

$$A_{sECFL}(\omega) = \frac{1}{\pi} \frac{\Gamma(\omega)}{\Gamma^2(\omega) + (\omega - \hat{k}v_F - h(\omega))^2} \times \left(1 - \frac{\omega}{\Delta} + c\hat{k}v_F\right)$$

$$\Gamma(\omega) = \frac{\omega^2 + \pi^2 T^2}{\omega_0} e^{-(\pi^2 T^2 + \omega^2)/\Omega_0^2}$$

$$\Gamma \rightarrow (\Gamma + \eta)$$

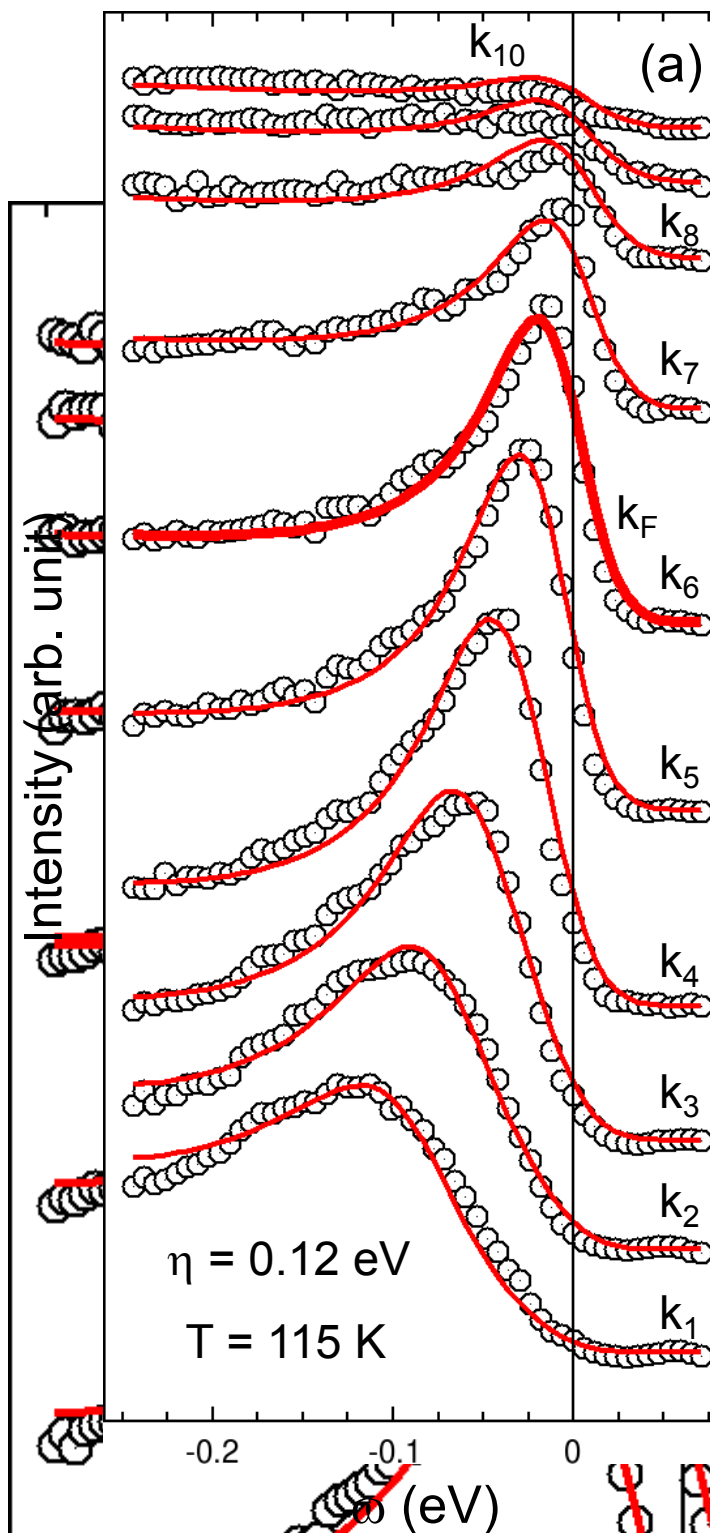
Energy dispersion and the 10 chosen values of  $k$  to compare theory and experiment.



Synchrotron ARPES data from J Campuzano's group compared to theory. BISSCO at optimal doping  $T = 115\text{K}$  along  $\langle 11 \rangle$  direction. Note that  $\eta = .12\text{ eV}$  (rather large)

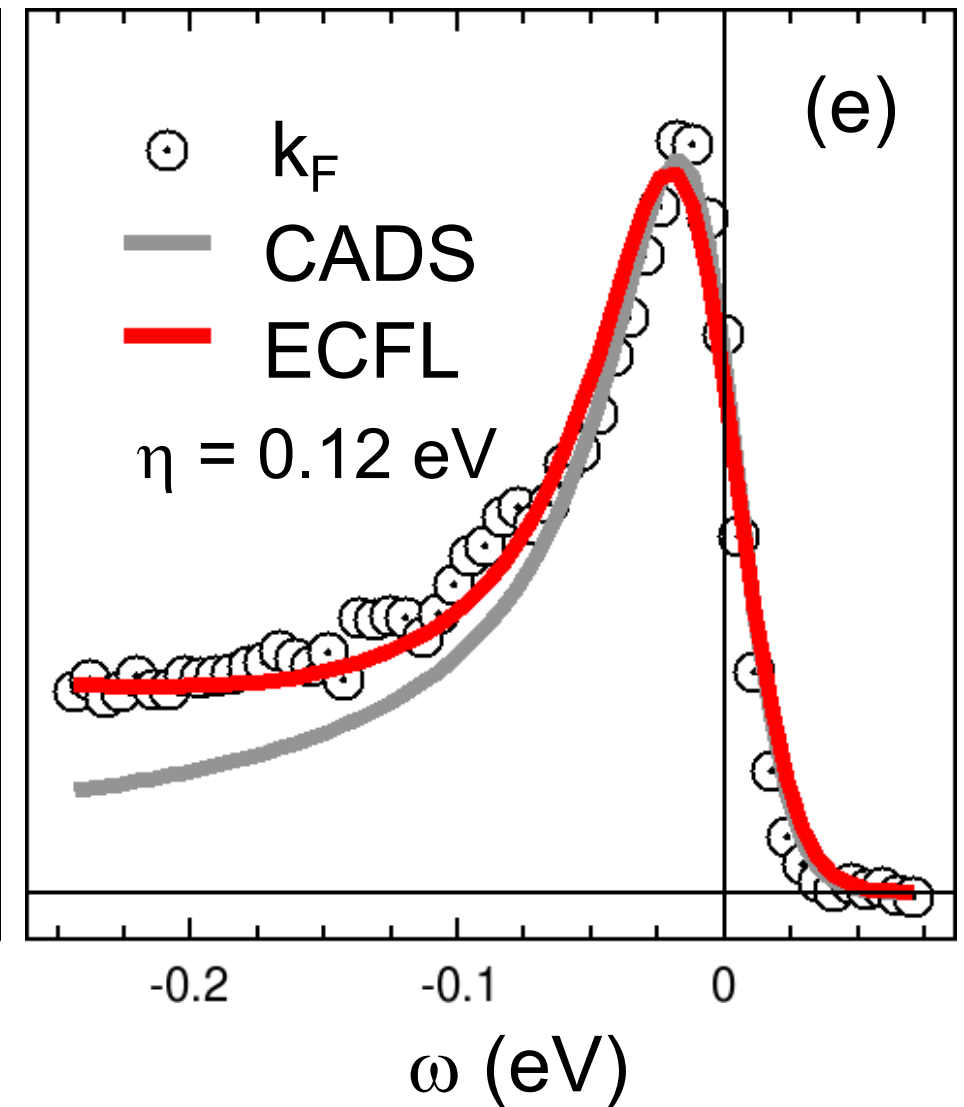
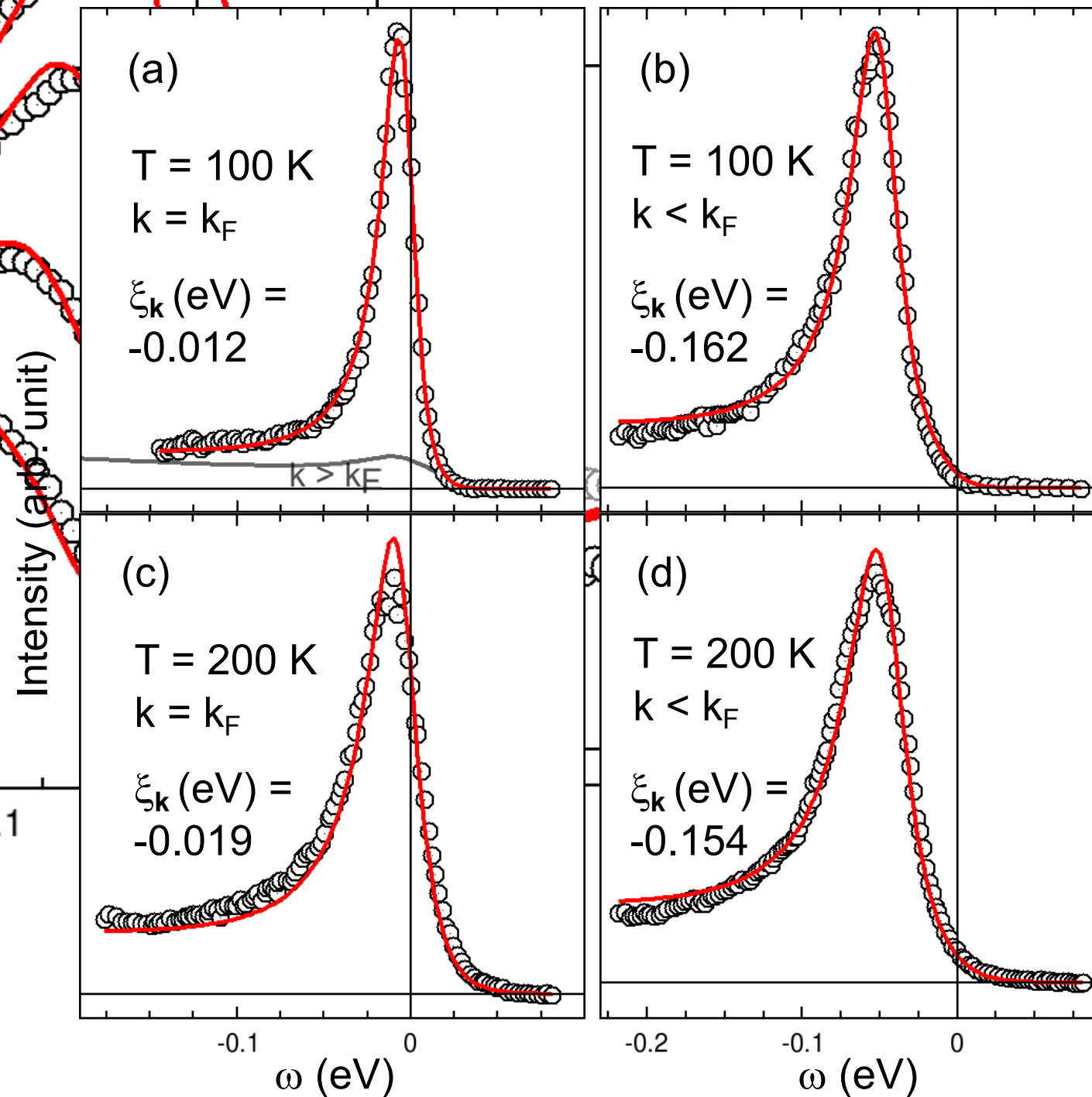
## Extremely Correlated Fermi-Liquid Description of Normal-State ARPES in Cuprates

G.-H. Gweon,<sup>1,\*</sup> B. S. Shastry,<sup>1,†</sup> and G. D. Gu<sup>2</sup>



Laser ARPES BISCO  
2212  $\eta = 0.032$  eV

Synchrotron ARPES BISCO 2212

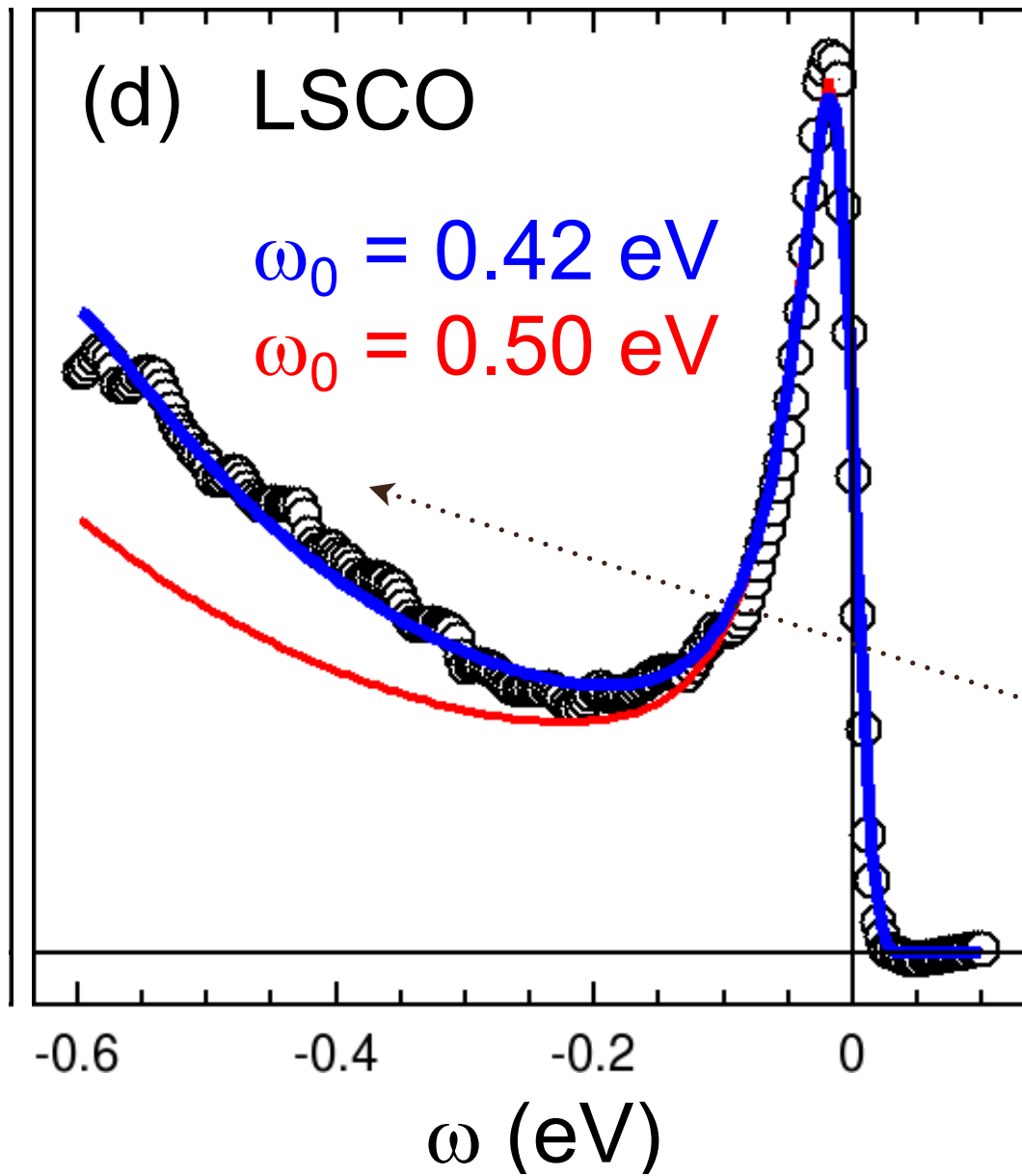


$\odot$   $\eta$  depends upon initial energy of photon-

$\odot$  Larger  $\eta$  for surface sensitive probe (HE Synchrotron Arpes)

$\odot$  small  $\eta$  for bulk sensitive probe (LASER Arpes)

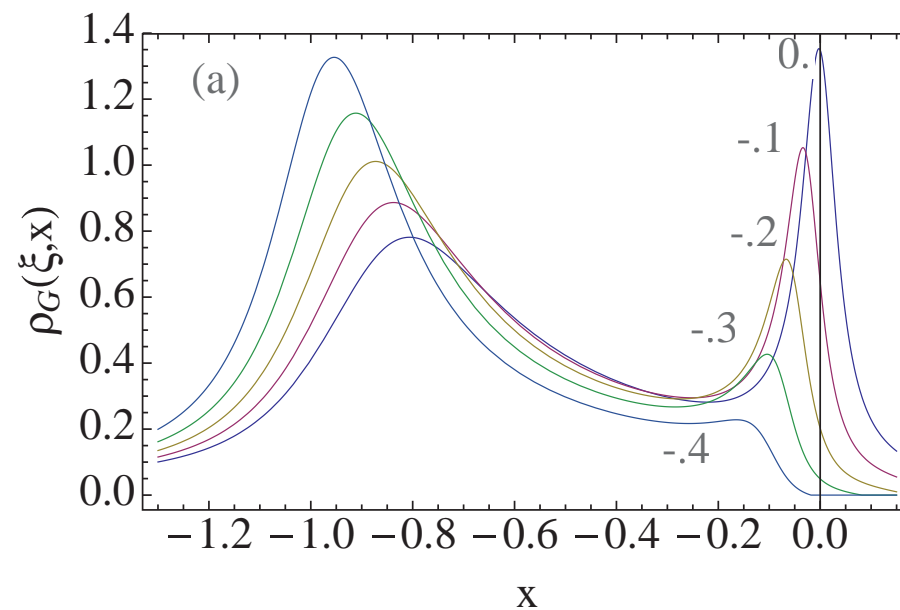
Same physical parameters only  $\eta$  different



Fujimori, ZX Shen et al

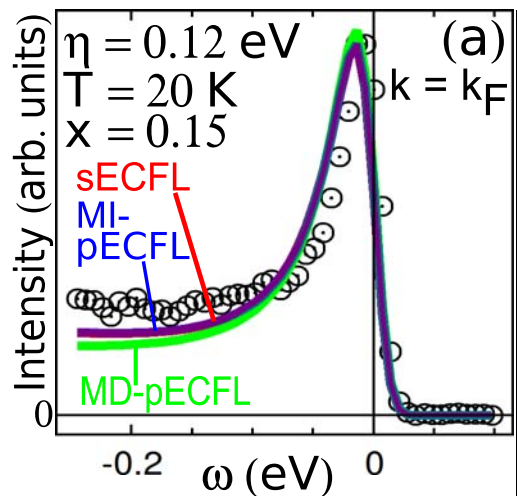
$$A(\vec{k}, \omega) = A_{FL}(\vec{k}, \omega) \left( 1 - \frac{n}{2} + \frac{n^2}{4} \cdot \frac{\xi_{\vec{k}} - \omega}{\Delta_0} \right)_+$$

**Smoking gun**  
Linear rise of intensity  
for occupied states.

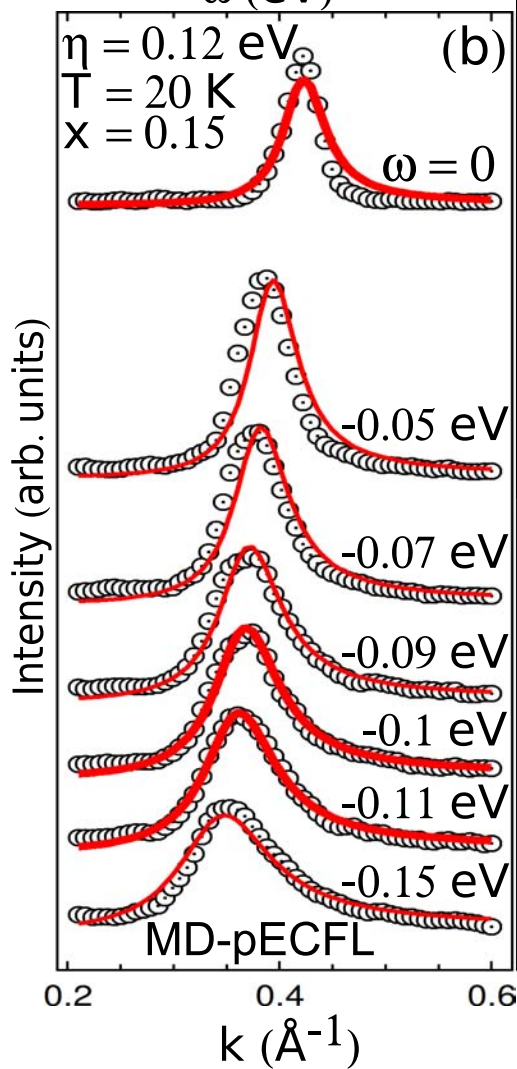


On a larger energy scale  
there are often broad peaks beyond which  
the intensity falls.

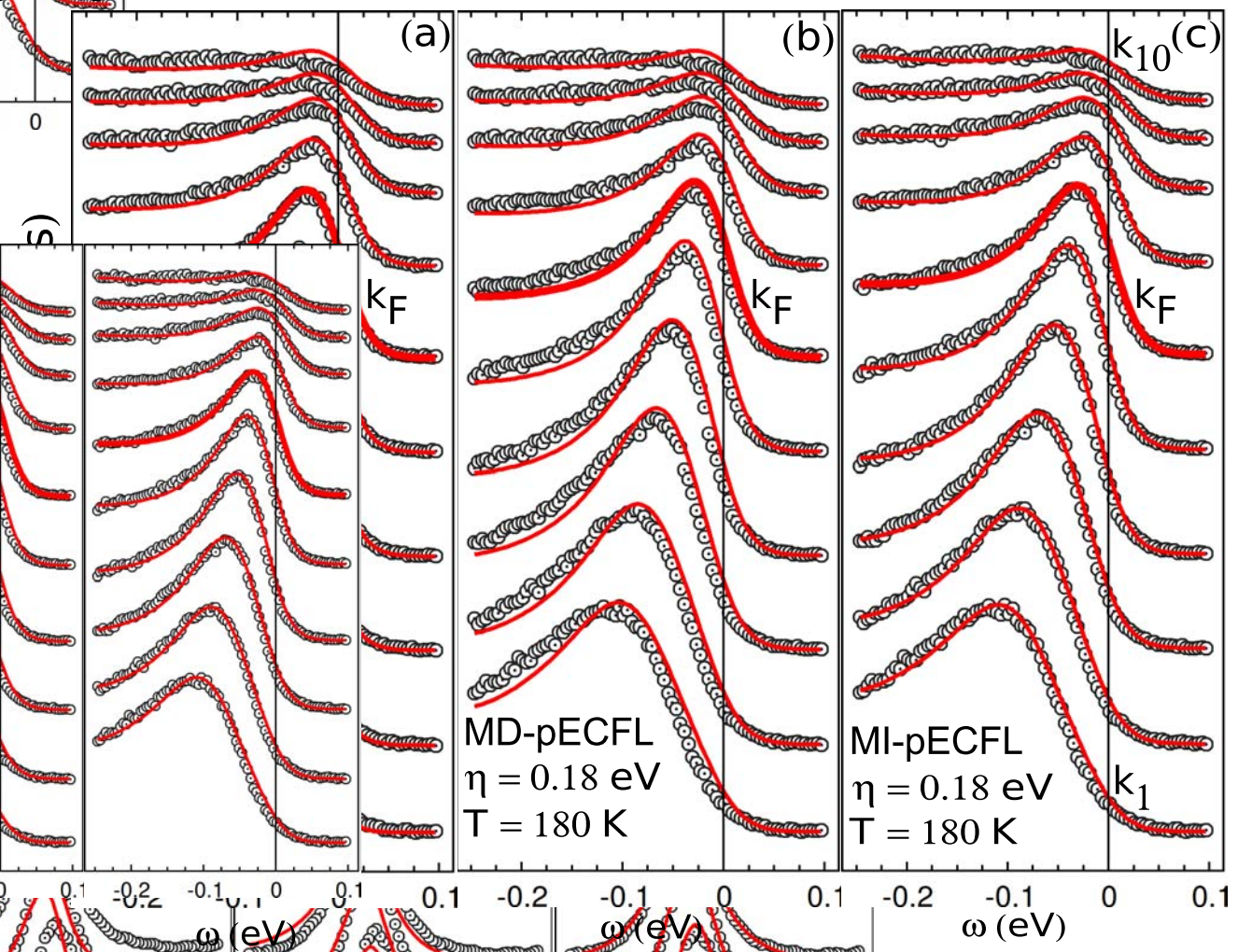
FIG. 4. EDC fits and MDC fits to the data of optimally doped ( $n = 0.85$ ) LSCO [26], taken along the nodal direction. (a)



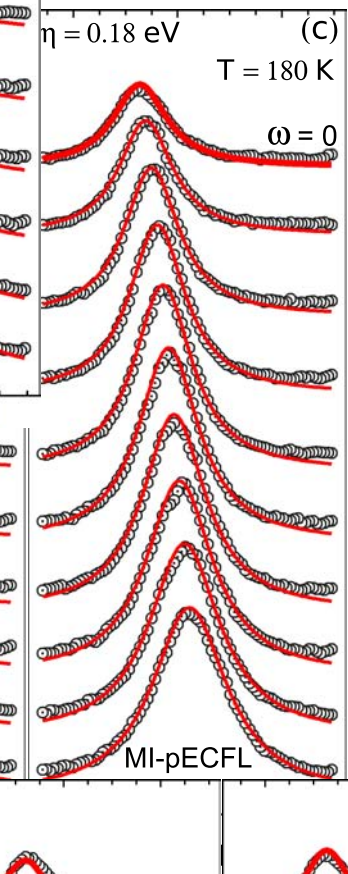
Can we fit both MDC and EDC's?  
Yes-



Line shape fits of EDCs for Bi2212 ( $x = 0.15$ )

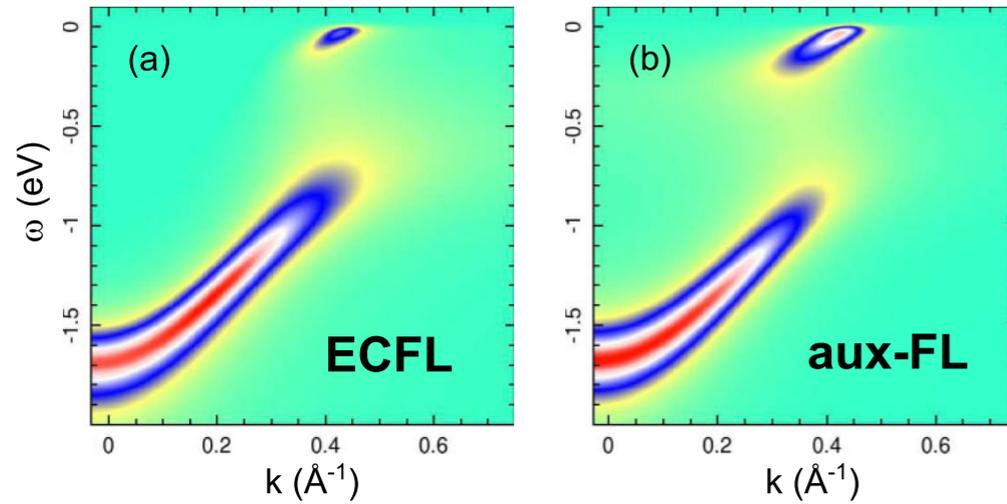


Line shape fits of MDCs for Bi2212 ( $x = 0.15$ )



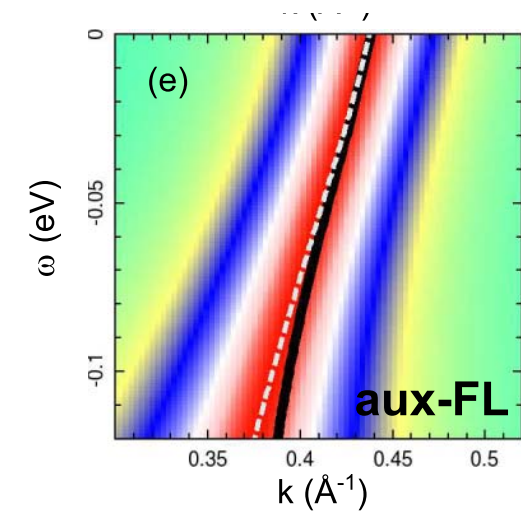
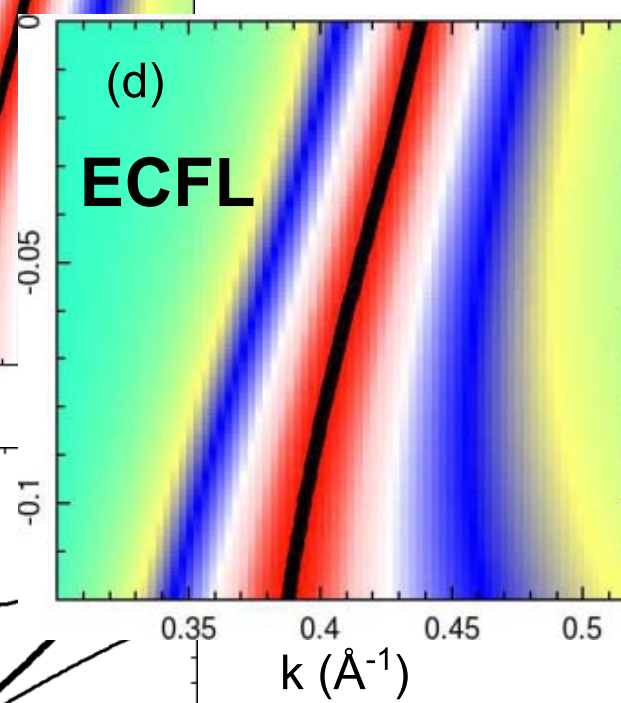
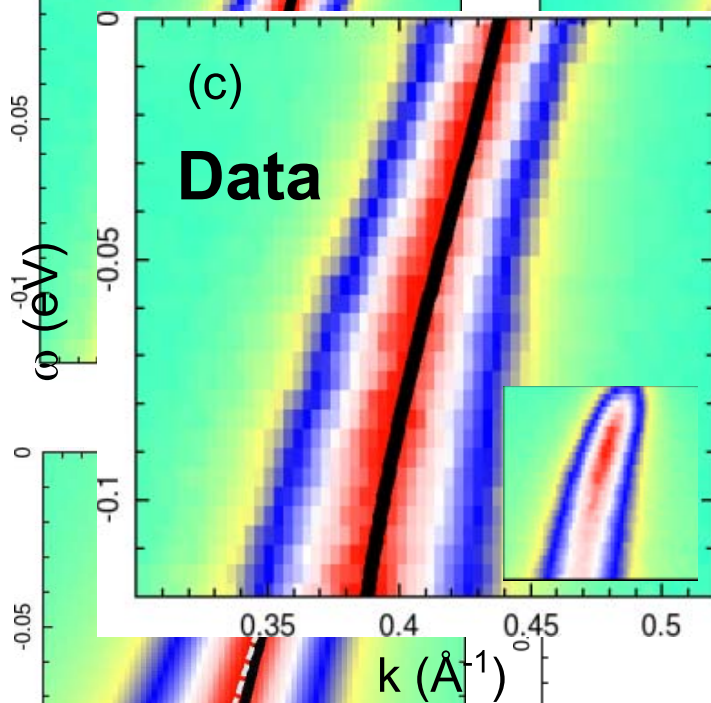
# Low energy and High kinks and ECFL

(MDC fits here)



H E Kink in both ECFL  
and auxiliary FL

L E Kink in ECFL at  $-0.05$  eV  
(not seen in aux-FL)



## Low energy kinks and their electronic origin. (non Landau FL)

$$A(\vec{k}, \omega) = \frac{z_0}{\pi} \frac{\Gamma_0}{(\omega - \nu_\Phi \hat{k} v_f)^2 + \Gamma_0^2} \times \mu(k, \omega)$$

$$\mu(\hat{k}, \omega) = 1 - \frac{\omega}{\Delta_0} + \frac{\nu_0 \hat{k} v_f}{\Delta_0},$$

$$\Gamma_0 = \eta + \frac{\pi^3 (k_B T)^2}{\Omega_\Phi}$$

$$Q(\hat{k}) = \Delta_0 + (\nu_0 - \nu_\Phi) \hat{k} v_f$$

$$r = \frac{\nu_0}{\nu_\Phi},$$

Q is a momentum variable  
r is the ratio of the two velocities  
 $\nu_0$  and  $\nu_\Phi$ .

Recall that  $\Delta_0$  is important asymmetry scale.

$$E(k) = \frac{1}{2-r} \left( \nu_\Phi \hat{k} v_f + \Delta_0 - \sqrt{r(2-r) \Gamma_0^2 + Q^2} \right),$$

$$E^*(k) = \left( \nu_0 \hat{k} v_f + \Delta_0 - \sqrt{\Gamma_0^2 + Q^2} \right).$$

$$E^*(k_{kink}) = -\frac{r}{r-1} \Delta_0 - \Gamma_0.$$

$$E(k_{kink}) = -\frac{1}{r-1} \Delta_0 - \Gamma_0 \sqrt{\frac{r}{2-r}},$$

Explicit expressions for both kink energies.

E and E\* are MDC and EDC peak energies found by max A w.r.t.  $\omega$  or k.

In MDC a clear maximum is not very robust. EDC more robust

Both spectra are hybrids of massless and massive Dirac spectra,

- asymptotically

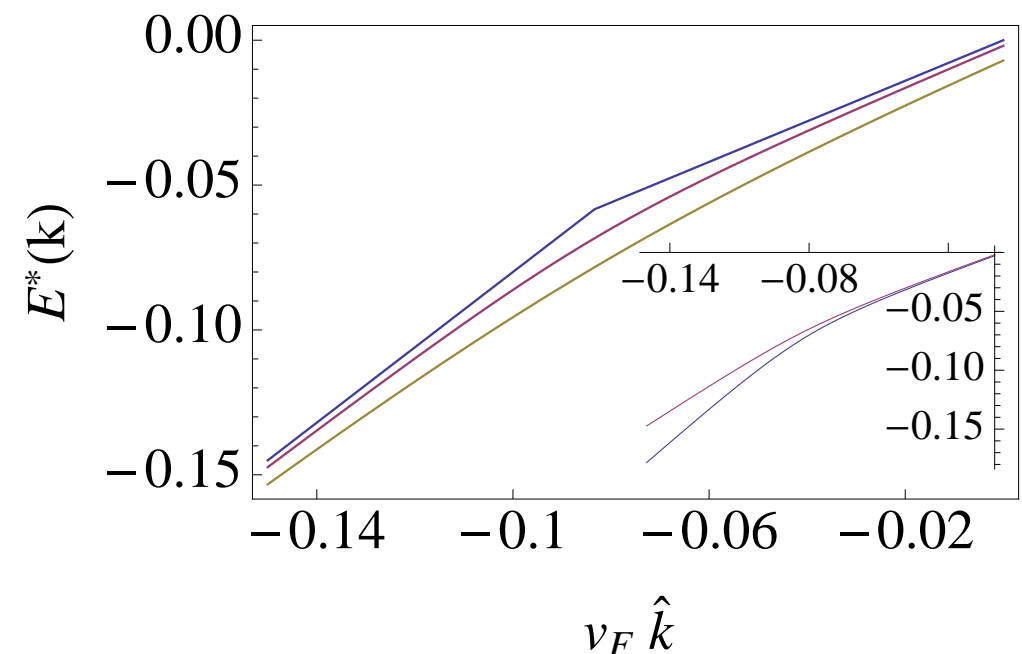
$$E(k) \sim \frac{1}{2-r} (\nu_\Phi + (\nu_0 - \nu_\Phi) \text{sign}(\hat{k})) \hat{k} v_f.$$

$$E^*(k) \sim (\nu_0 + (\nu_0 - \nu_\Phi) \text{sign}(\hat{k})) \hat{k} v_f$$

Both spectra have kinks at  $Q=0$  i.e.

$$(\hat{k} v_f)_{kink} = \frac{\Delta_0}{\nu_\Phi (1-r)},$$

Hence kink in occupied side provided  $r > 1$ .



LE Kink arises from role of comparison function.

Kink energy reads off important and emergent asymmetry energy scale  $\Delta_0$ .

Dependence on n, T and  $\eta$  given explicitly here

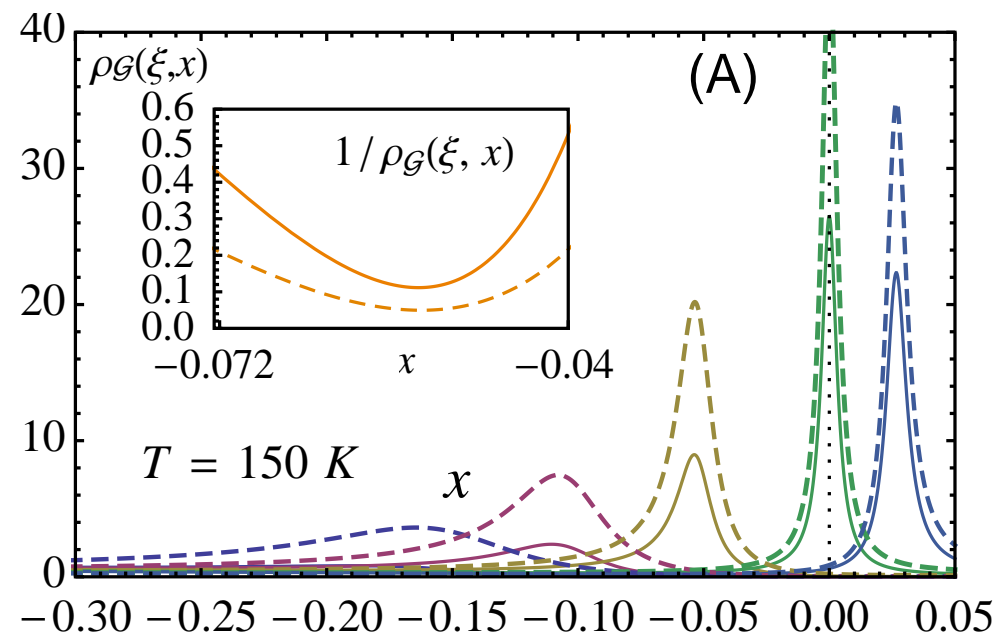
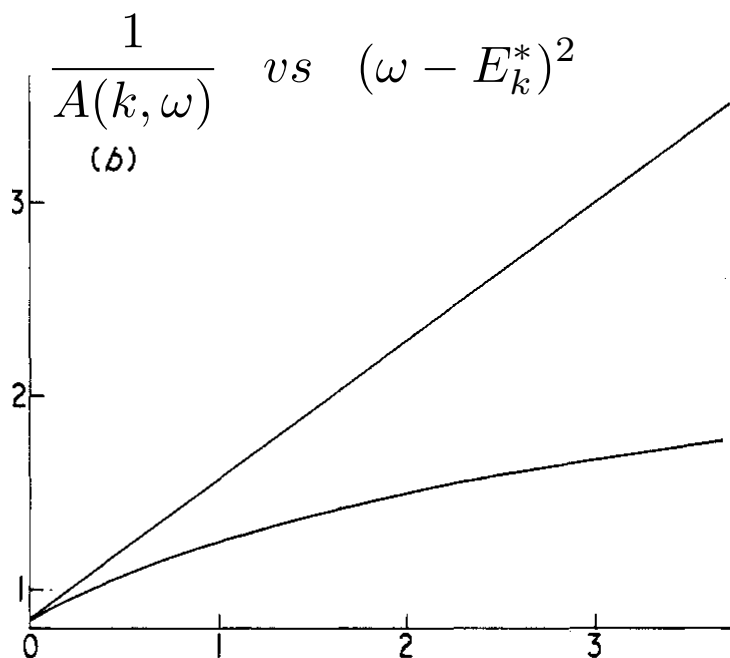
# Identifying Asymmetry at lowest frequencies in ARPES data:

Main message:

Inverse intensity gives a better perspective for identifying asymmetry.

Intensity itself focusses attention elsewhere.

Doniach Sunjic 1969!!



Shastry, Phys. Rev. Letts (2011)

ECFL line shape (and ACDS) predicts that

$$Q(\tilde{\omega}_k) = \frac{\tilde{\omega}_k^2}{A(k, E_k^*)/A(k, E_k^* + \tilde{\omega}_k) - 1}$$

$$Q(\tilde{\omega}_k) = A - B \tilde{\omega}_k$$

Construct object Q from intensity

$$\tilde{\omega}_k = \omega - E_k^*,$$

energy shifted by peak position

A sloping Q factor pinpoints and quantifies asymmetry!

# Some predictions re asymmetry

Dynamical P-H transformation  $(\hat{k} \equiv \vec{k} - \vec{k}_F)$

$$(\hat{k}, \omega) \rightarrow -(\hat{k}, \omega).$$

$$\mathcal{S}_G(\vec{k}, \omega) \equiv f(\omega)f(-\omega)\rho_G(\vec{k}, \omega) = \frac{1}{|M(\vec{k})|} f(-\omega)I(\vec{k}, \omega).$$

This is the Fermi symmetrized spectral function that focuses attention near chemical potential. Here  $I(k, \omega)$  is ARPES intensity and  $M$  is dipole matrix element

Construct symmetric and antisymmetric combinations under the above DPH transformation

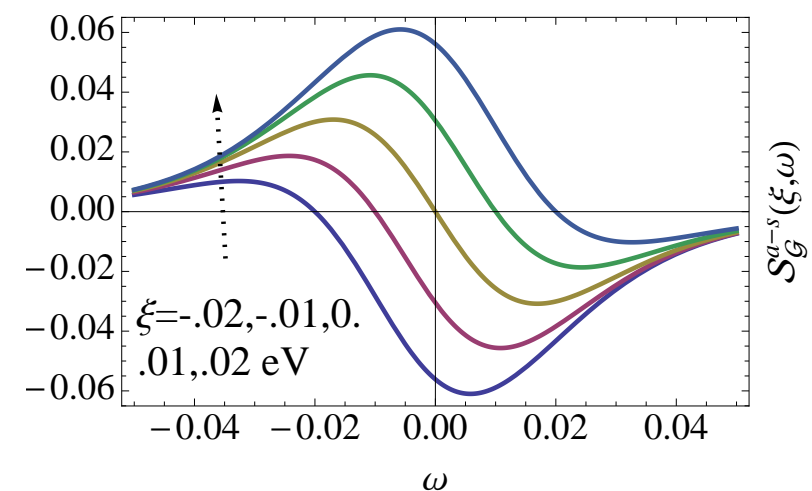
$$\frac{1}{2} \left[ \mathcal{S}_G(\vec{k}_F + \hat{k}, \omega) \mp \mathcal{S}_G(\vec{k}_F - \hat{k}, -\omega) \right]$$

From these form the (dimensionless) asymmetry ratio  $R$

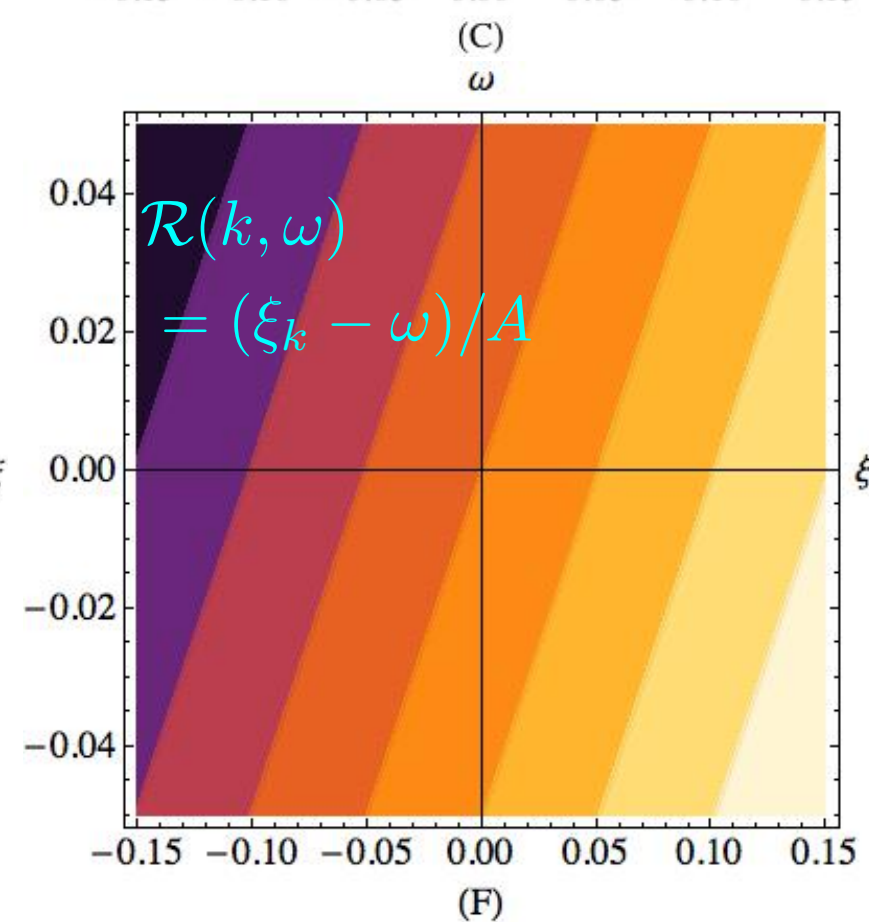
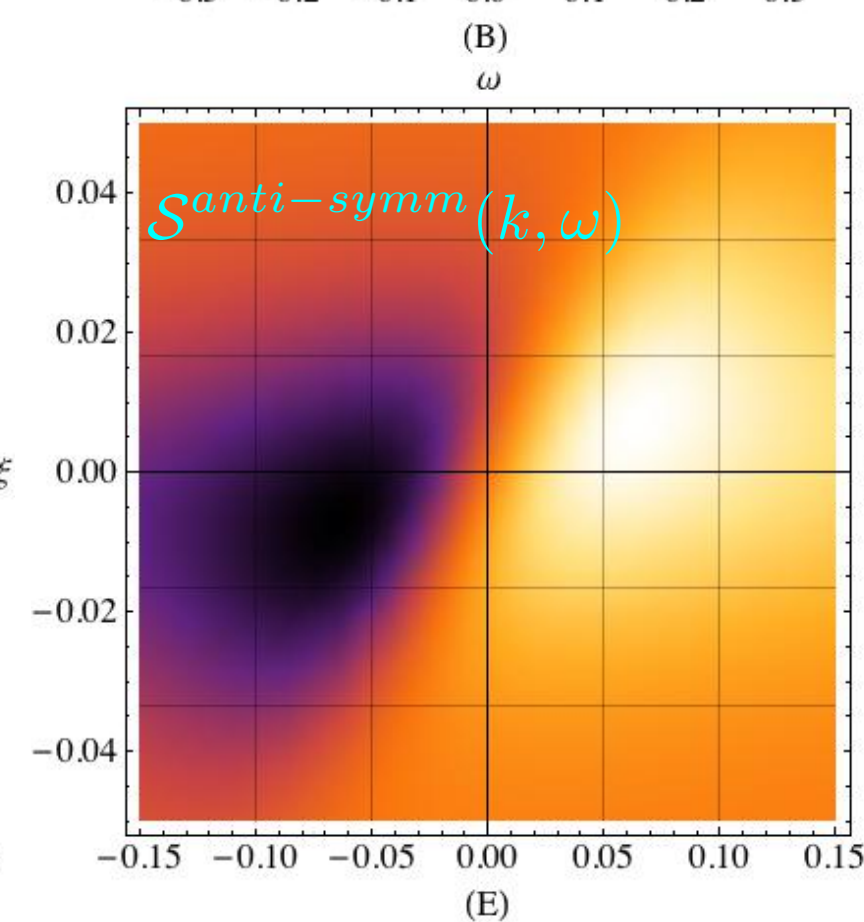
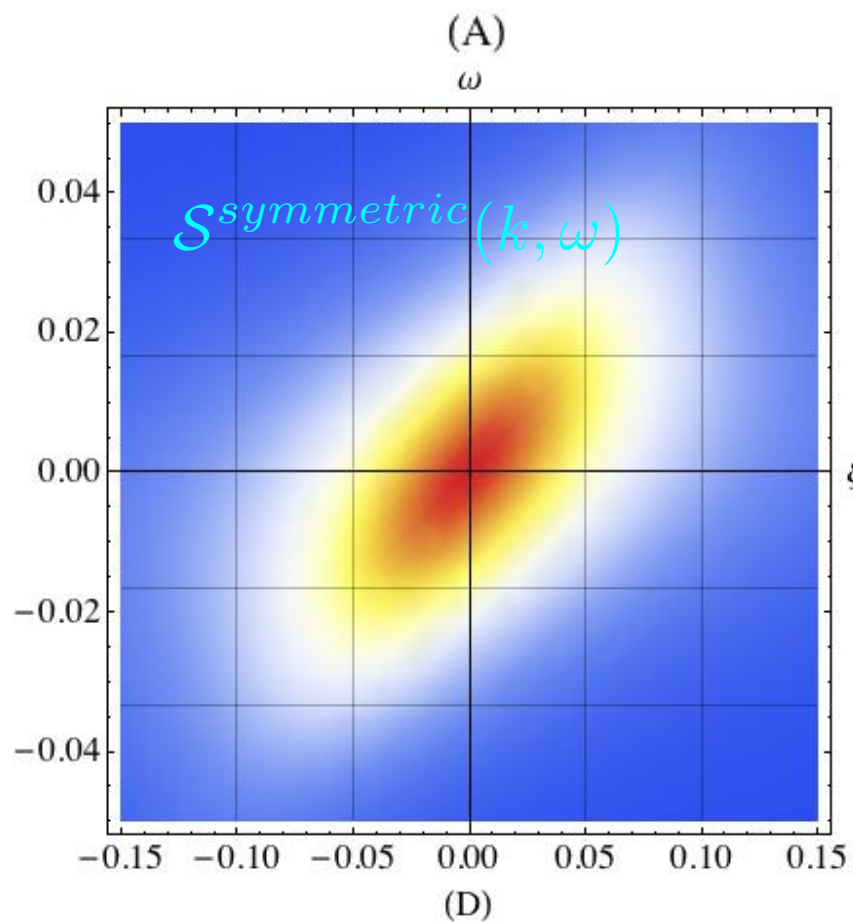
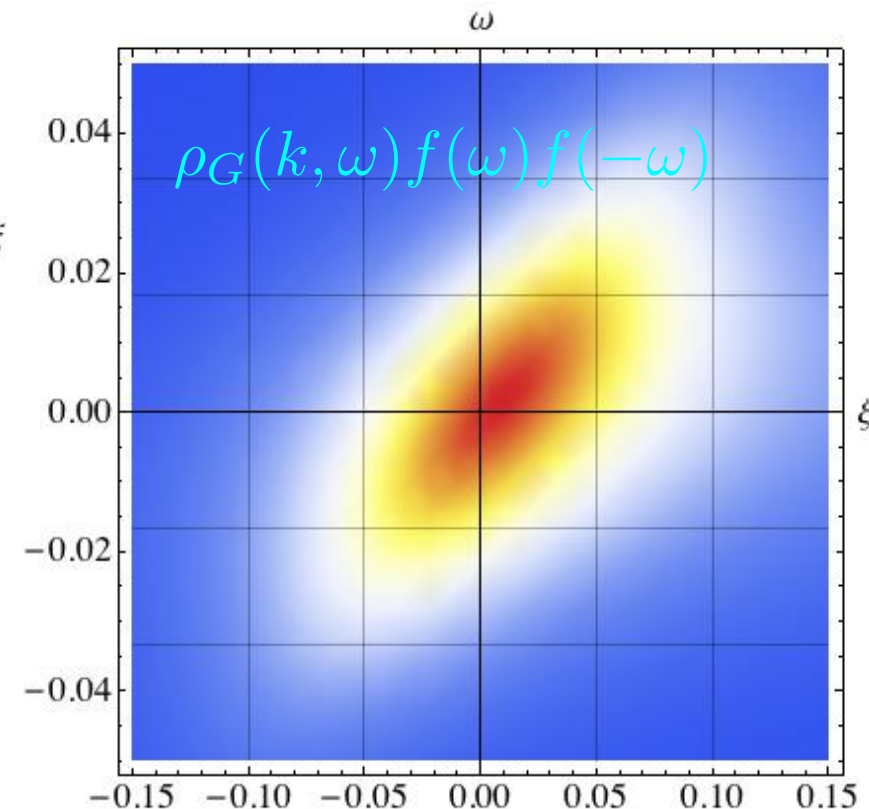
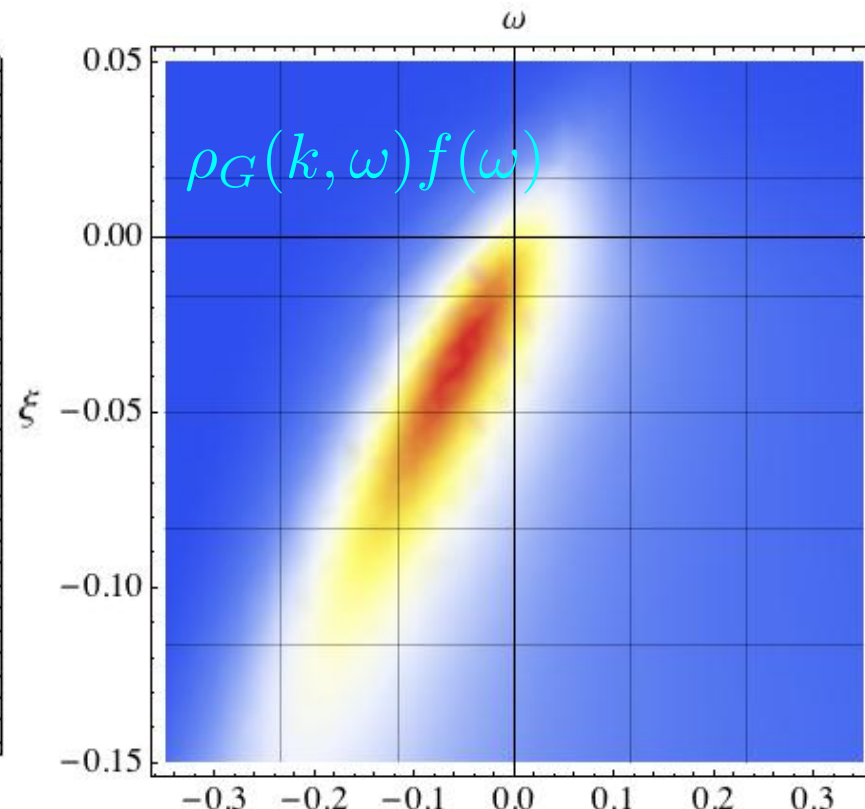
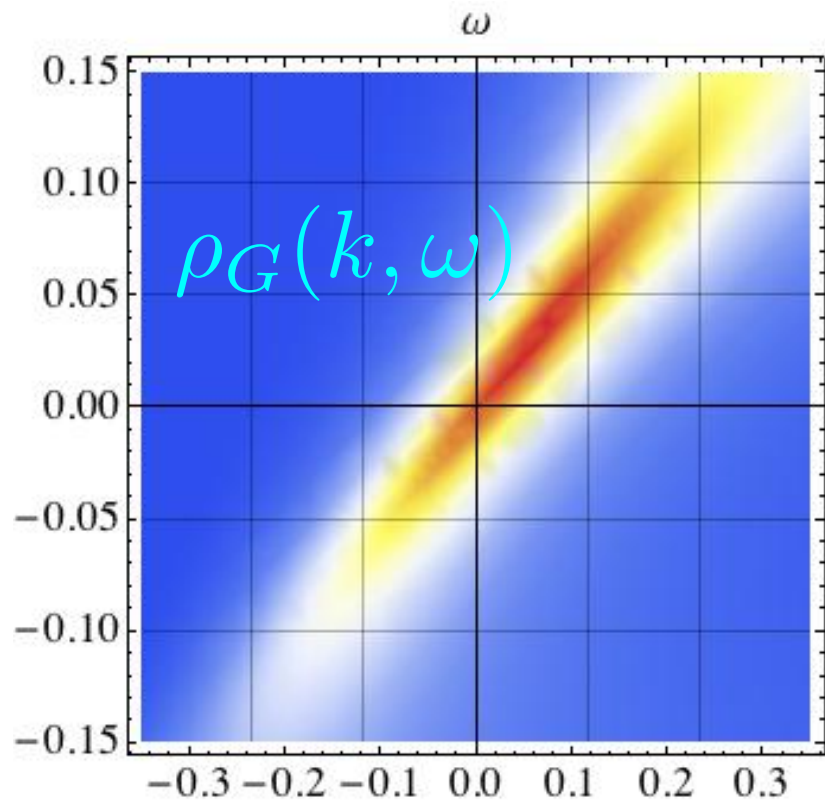
$$\mathcal{R}_G(\vec{k}_F | \hat{k}, \omega) = \mathcal{S}_G^{a-s}(\vec{k}_F | \hat{k}, \omega) / \mathcal{S}_G^s(\vec{k}_F | \hat{k}, \omega)$$

Important ratio  
Can experimentally distinguish between two classes of theories.

Simplified ECFL



Scale of  $\omega$  is eV. Enormous asymmetry is



Requires momentum resolution  $\Delta k = .001$  Angstrom (perhaps just beyond current reach.)

### *Asymmetry related comments:*

- Experimentally feasible if momentum resolution is attained (not too far from current resolution-).
- ECFL and Anderson Casey have similar features. A-C line shapes share the feature of non trivial asymmetry of  $O(1)$  on fairly small energy scale ( $\sim 25$  meV). If  $\Delta_0 \rightarrow (kT)$  then ECFL  $\sim$  CADS!
- Fermi liquids do not have such large asymmetries on a similarly small energy scale.
- Marginal Fermi Liquids and Almost AFM Fermi liquids are all particle hole **symmetric**.
- This can be used to discriminate between classes of theories.

### *Prospects and Open issues*

- Superconductivity due to exchange J - this is very natural - (MS in preparation)
- Nature of Mott insulating state?
- Underdoped phase?
- Other broken symmetries (AFM- Quantum liquids..)?

*Merci Beaucoup*